RESEARCH ARTICLE

AMERICAN JOURNAL OF medical genetics PART A

The Spectrum of *ZEB2* Mutations Causing the Mowat–Wilson Syndrome in Japanese Populations

**Yasukazu Yamada,[1] Noriko Nomura,[1] Kenichiro Yamada,[1] Mari Matsuo,[2] Yuka Suzuki,[3] Kiyoko Sameshima,[4] Reiko Kimura,[1] Yuto Yamamoto,[5] Daisuke Fukushi,[1] Yayoi Fukuhara,[1] Naoko Ishihara,[6] Eriko Nishi,[7] George Imataka,[8] Hiroshi Suzumura,[8] Shin-Ichiro Hamano,[9] Kenji Shimizu,[10] Mie Iwakoshi,[11] Kazunori Ohama,[12] Akira Ohta,[13] Hiroyuki Wakamoto,[14] Mitsuharu Kajita,[15] Kiyokuni Miura,[16] Kenji Yokochi,[17] Kenjiro Kosaki,[18] Tatsuo Kuroda,[19] Rika Kosaki,[20] Yoko Hiraki,[21] Kayoko Saito,[2] Seiji Mizuno,[7] Kenji Kurosawa,[22] Nobuhiko Okamoto,[5] and Nobuaki Wakamatsu[1]*

[1]Department of Genetics, Institute for Developmental Research, Aichi Human Service Center, Kasugai, Aichi, Japan

[2]Institute of Medical Genetics, Tokyo Women's Medical University, Shinjuku, Tokyo, Japan

[3]Department of Community Emergency Medicine, Graduate School of Medicine Ehime University, Tohon, Ehime, Japan

[4]Department of Medical Genetics, Gunma Children's Medical Center, Shibukawa, Gunma, Japan

[5]Department of Medical Genetics, Osaka Medical Center and Research Institute for Maternal and Child Health, Izumi, Osaka, Japan

[6]Department of Pediatrics, Nagoya University Graduate School of Medicine, Nagoya, Aichi, Japan

[7]Department of Pediatrics, Central Hospital, Aichi Human Service Center, Kasugai, Aichi, Japan

[8]Department of Pediatrics, Dokkyo Medical University School of Medicine, Shimotsuga, Tochigi, Japan

[9]Division of Neurology, Saitama Children's Medical Center, Saitama, Saitama, Japan

[10]Division of Medical Genetics, Saitama Children's Medical Center, Saitama, Saitama, Japan

[11]Department of Healthcare Science, Kobe-Tokiwa University, Kobe, Hyogo, Japan

[12]Department of Pediatric Surgery, Ishikawa Prefectural Central Hospital, Kanazawa, Ishikawa, Japan

[13]Department of Pediatrics, Shikoku Medical Center for Children and Adults, Zentsuji, Kagawa, Japan

[14]Department of Pediatrics, Ehime Rehabilitation Center for Children, Tohon, Ehime, Japan

[15]Department of Pediatrics, Toyota Kosei Hospital, Toyota, Aichi, Japan

[16]Division of Developmental Disability Medicine, Nagoya University Graduate School of Medicine, Nagoya, Aichi, Japan

[17]Department of Pediatric Neurology, Seirei-Mikatahara General Hospital, Hamamatsu, Shizuoka, Japan

[18]Center for Medical Genetics, Keio University School of Medicine, Shinjuku, Tokyo, Japan

[19]Department of Pediatric Surgery, Keio University School of Medicine, Shinjuku, Tokyo, Japan

[20]Division of Medical Genetics, National Center for Child Health and Development, Setagaya, Tokyo, Japan

[21]Hiroshima Municipal Center for Child Health and Development, Hiroshima, Hiroshima, Japan

[22]Division of Medical Genetics, Kanagawa Children's Medical Center, Yokohama, Kanagawa, Japan

Manuscript Received: 20 November 2013; Manuscript Accepted: 27 February 2014

Mowat–Wilson syndrome (MWS) is a multiple congenital anomaly syndrome characterized by moderate or severe intellectual disability, a characteristic facial appearance, microcephaly, epilepsy, agenesis or hypoplasia of the corpus callosum, congenital heart defects, Hirschsprung disease, and urogenital/renal anomalies. It is caused by de novo heterozygous loss of function mutations including nonsense mutations, frameshift mutations, and deletions in *ZEB2* at 2q22. *ZEB2* encodes the zinc finger E-box binding homeobox 2 protein consisting of 1,214 amino acids. Herein, we report 13 nonsense and 27 frameshift mutations from

Conflict of interest: The authors declare that they have no conflict of interests.

Grant sponsor: Takeda Science Foundation; Grant sponsor: Health Labor Sciences Research Grant.

*Correspondence to:
Nobuaki Wakamatsu, M.D., Ph.D., Department of Genetics, Institute for Developmental Research, Aichi Human Service Center, 713-8 Kamiya-cho, Kasugai, Aichi 480-0392, Japan.
E-mail: nwaka@inst-hsc.jp

Article first published online in Wiley Online Library (wileyonlinelibrary.com): 00 Month 2014
DOI 10.1002/ajmg.a.36551

40 newly identified MWS patients in Japan. Although the clinical findings of all the Japanese MWS patients with nonsense and frameshift mutations were quite similar to the previous review reports of MWS caused by nonsense mutations, frameshift mutations and deletions of *ZEB2*, the frequencies of microcephaly, Hirschsprung disease, and urogenital/renal anomalies were small. Patients harbored mutations spanning the region between the amino acids 55 and 1,204 in wild-type ZEB2. There was no obvious genotype–phenotype correlation among the patients. A transfection study demonstrated that the cellular level of the longest form of the mutant ZEB2 protein harboring the p.D1204Rfs*29 mutation was remarkably low. The results showed that the 3′-end frameshift mutation of *ZEB2* causes MWS due to ZEB2 instability.

Key words: Mowat–Wilson syndrome; frameshift mutation; nonsense mutation; ZEB2

How to Cite this Article:
Yamada Y, Nomura N, Yamada K, Matsuo M, Suzuki Y, Sameshima K, Kimura R, Yamamoto Y, Fukushi D, Fukuhara Y, Ishihara N, Nishi E, Imataka G, Suzumura H, Hamano S-I, Shimizu K, Iwakoshi M, Ohama K, Ohta A, Wakamoto H, Kajita M, Miura K, Yokochi K, Kosaki K, Kuroda T, Kosaki R, Hiraki Y, Saito K, Mizuno S, Kurosawa K, Okamoto N, Wakamatsu N. 2014. The spectrum of *ZEB2* mutations causing the Mowat–Wilson syndrome in Japanese populations.
Am J Med Genet Part A 9999:1–10.

INTRODUCTION

Mowat et al. [1998] described six patients with severe intellectual disability, a distinct facial appearance, microcephaly, short stature, and Hirschsprung disease as a new syndrome. The authors also suggested that the disease locus was located at 2q22-23, because their only patient and a previously reported similar patient [Lurie et al., 1994] had deletions at 2q21-23 and 2q22-23, respectively. The determination of the chromosomal translocation breakpoint from two patients harboring the 2q22 translocation led to the identification of the zinc finger E-box binding homeobox 2 gene (*ZEB2*, also known as *ZFHX1B* and *SIP1*) as the disease gene [Cacheux et al., 2001; Wakamatsu et al., 2001]. Mowat–Wilson syndrome (MWS: OMIM#235730) was established as a distinct and recognizable syndrome; in particular, the characteristic facial appearance, which includes frontal bossing, eyebrows with medially flaring, hypertelorism, telecanthus, a broad nasal bridge, prominent columella, a prominent chin, and anomalies of ears, was associated with loss of function mutations (e.g., nonsense mutations, frameshift mutations, and deletions) in one allele of *ZEB2* [Zweier et al., 2002; Mowat et al., 2003]. Numerous reports (approximately 200) of *ZEB2* mutations in MWS [for clinical summaries or a review, see Zweier et al., 2005; Dastot-Le Moal et al., 2007; Garavelli et al., 2009] have been described. There is no obvious genotype–phenotype correlation in the MWS patients showing loss of function *ZEB2* mutations except for two patients with large deletions (>10 Mb) at the 2q22-24 locus, who presented with quite severe conditions and different original cases [Zweier et al., 2003; Ishihara et al., 2004]. MWS is caused by de novo mutations in one allele of *ZEB2*. The parents of MWS patients are usually healthy, and genetic abnormalities including apparent somatic mosaicism have not been reported. However, four families with MWS in siblings have been reported to be likely caused by germ-line mosaicism [McGaughran et al., 2005; Zweier et al., 2005; Cecconi et al., 2008; Ohtsuka et al., 2008].

ZEB2 is a member of the family of the two-handed zinc finger/homeodomain proteins containing an SMAD-binding domain (p.437–487), a homeodomain-like sequence (p.651–700), and two separate clusters of zinc fingers: an N-terminal domain (p.213–304) and a C-terminal domain (p.1001–1076) [Verschueren et al., 1999]. ZEB2 also possesses domains that interact with the nucleosome remodeling and histone deacetylation (NuRD) complex (p.14–17, 20) [Verstappen et al., 2008] and the transcriptional co-repressor C-terminal binding protein (p.757–863) [Postigo et al., 2003]. Recently, several Zeb2 functions in neuronal development and maturation have been identified by analyzing conditional knockout mice. Firstly, Zeb2 regulates the production of signals from post-mitotic cells back to the germinal zone to ensure the sequential generation of appropriate numbers of different neurons and glial cells throughout corticogenesis [Seuntjens et al., 2009]. Secondly, Zeb2 is essential for central nervous system myelination through the modulation of two distinct regulatory pathways (i.e., BMP-Smad and Wnt-β-catenin pathways) [Weng et al., 2012]. Thirdly, Zeb2 promotes a fate switch between cortical and striatal interneuron lineages through the repression of Nkx2-1 during neuronal migration from the medial ganglionic eminence [McKinsey et al., 2013].

Here, we report on nonsense and frameshift *ZEB2* mutations and the clinical features of 40 newly identified MWS patients in Japan. One patient carries the frameshift mutation of p.D1204Rfs*29 at the C-terminal of *ZEB2*; the mutant ZEB2 shares 99% (1,203/1,214) of its amino acids with the wild-type protein. We analyze the C-terminal mutant of ZEB2 and discuss the pathogenesis of the disease.

MATERIALS AND METHODS

Clinical Studies of MWS

Written informed consent was obtained from all the participants of this study. The experiments were conducted after approval by the Institutional Review Board at the Institute for Developmental Research, Aichi Human Service Center. The patients participating in this study were labeled S-001–S-131, except for five patients (K-01, K-02, O-01, P-1, P-2), whose *ZEB2* analysis was separately performed. S-073 (a-c) are sibling cases. The clinical and molecular analysis of *ZEB2* from S-001–S-042, S-073 (a-c), and P-1 and P-2 have been published elsewhere [Wakamatsu et al., 2001; Yamada

et al., 2001; Ishihara et al., 2004; Sasongko et al., 2007; Ohtsuka et al., 2008]. We performed the genetic analysis of the *ZEB2* in Japanese patients with a potential clinical diagnosis of MWS and presented the confirmed MWS cases based on *ZEB2* analysis at the corresponding meetings of physicians in charge by supporting the Research on Measures for Intractable Diseases sponsored by the Ministry of Health Labor and Welfare in Japan. The prevalence of MWS was determined by epidemiological survey of the patients from the hospitals and medical centers for pediatric rehabilitation at the Aichi and Kanagawa prefectures.

DNA Sequencing

Genomic DNA was isolated from the peripheral blood of the patients with a possible clinical diagnosis of MWS and the mutations in *ZEB2* were evaluated as previously described [Yamada et al., 2001]. Briefly, nine PCR products encompassing all nine coding exons (exons 2–10) including intron/exon boundaries were amplified and sequenced directly. To confirm the mutations detected in one allele of the patients, the PCR products were subcloned into pGEM-T Easy (Promega, Madison, WI) and sequenced. The nucleotide sequence of the DNA fragment was determined using the GenomeLab™ GeXP Genetic Analysis System (Beckman Coulter, Fullerton, CA), with the GenomeLab™ Dye Terminator Cycle Sequencing with Quick Start Kit (Beckman Coulter).

Construction of the Wild-Type and Mutant ZEB2 Expression Vectors

Wild-type ZEB2 cDNA was amplified from the first-strand cDNA prepared from HEK293 cells using the specific primer pair S1-A1 (S1, exon 1: 5′-cgctgaattcaatgaagcagccgatcatg-3′; A1, exon 10: 5′-aatgctctagattattacatgccatc-3′). An *Eco*RI recognition site (gaattc) or an *Xba*I recognition site (tctaga) was introduced into S1 or A1, respectively. After confirming the nucleotide sequences, the *Eco*RI/*Xba*I fragment of the wild-type ZEB2 cDNA was subcloned into the *Eco*RI/*Xba*I site of a mammalian expression vector, p3xFLAG-CMV (Sigma–Aldrich, St. Louis, MO) (pFLAG-ZEB2). To generate the D1204Rfs*29 mutant of ZEB2, the 3′ portion of the *ZEB2* was amplified with the primer pair S2-A2 (S2, exon 10: 5′-cgggcttacttgcagagcat-3′; A2, exon 10: 5′-catgaacagcttaactctagagtgttttc-3′) using the genomic DNA prepared from the patient's peripheral blood cells. An *Xba*I recognition site was introduced into A2. A 189-bp piece of the *Bam*HI/*Xba*I fragment of pFLAG-ZEB2 was exchanged with a 184-bp piece of *Bam*HI/*Xba*I-digested PCR fragment (pFLAG-ZEB2-D1204Rfs*29). Similarly, the ZEB2 expression vectors (pFLAG-ZEB2-D1204X and pFLAG-ZEB2-M1210X) containing premature termination codons at the 3′-end were generated by in vitro mutagenesis. The nucleotide sequences of all the constructed ZEB2 expression vectors were verified by sequencing.

Expression Study of Wild-Type and Mutant ZEB2 Proteins in HEK293 Cells

Each ZEB2 expression vector (4 μg; p3xFLAG-CMV, pFLAG-ZEB2, pFLAG-ZEB2-D1204Rfs, pFLAG-ZEB2-D1204X, and pFLAG-ZEB2-M1210X) was cotransfected with 50 ng of pCMV-β-gal (an *Escherichia coli* β-galactosidase expression vector) into HEK293 cells in six-well dishes using the Lipofectamine 2000 reagent (Invitrogen, Carlsbad, CA). After a 24-h transfection, the cells from each well were harvested and replated in two wells of six-well dishes. After a 48-h transfection, the cells from one of the two wells were washed with PBS, solubilized with a lysis buffer containing 20 mM Tris–HCl (pH 7.5) and Protease Inhibitor Cocktail (1:1,000 dilution), and sonicated using SOMIFIER 250 (BRANSON, Danbury, CT). The FLAG tagged ZEB2 mRNA levels relative to mRNA of β-actin (ACTB) were analyzed by the multiplex PCR method [Ishihara et al., 2004]. Total RNA was extracted from HEK293 cells transfected with each of the ZEB2-expressing vectors using TRIzol Reagent (Invitrogen) and first-strand cDNAs were synthesized by reverse transcription of 4.5 μg of total RNA using First-Strand cDNA Synthesis Kit (GE Healthcare, Tokyo, Japan). Primer pairs were designed to amplify a 178-bp fragment (90-bp of FLAG and 88-bp of ZEB2) of FLAG tagged ZEB2 cDNA: S3 (sense primer for the FLAG sequence), 5′-aaccatggactacaaagacca-3′ and A3 (antisense primer for exons 1 and 2 of ZEB2), 5′-cattgtcatagttcaccacgt-3′, and a 149-bp fragment of ACTB: S4, 5′-gacaggatgcagaaggagat-3′ and A4, 5′-ctgcttgctgatccacatct-3′. Aliquots (equivalent to 0.1 μg of total RNA) of first-strand cDNA were amplified by PCR in a total volume of 20 μl, each containing 0.3 μM of the both primer pairs (S3-A3 and S4-A4), and 20 cycles were performed. PCR products were separated on 1.5% low melting point agarose gel electrophoresis. Western blotting was performed using an anti-FLAG M2 antibody (1:6,000 dilution; Sigma–Aldrich) following the same method as described elsewhere [Yamada et al., 2013]. Proteins were analyzed using ImageQuant LAS 4000 mini (GE Healthcare). The efficiency of the DNA transfection was verified by measuring the *E. coli* β-galactosidase activity using O-nitrophenyl-β-D-galactopyranoside (ONPG) as the substrate.

RESULTS

The Prevalence of MWS

The epidemiological survey demonstrated that the prevalence of MWS at the Aichi and Kanagawa prefectures is 1:74,000 and 1:110,000, respectively. Thus, similar to the results of a previous report [Evans et al., 2012], the prevalence of MWS in Japan is approximately 1:90,000.

Identification of Nonsense and Frameshift Mutations in *ZEB2*

We have identified nonsense mutations in 13 new patients (Table I). The mutation p.R695X, which was previously reported in eight patients [Ishihara et al., 2004; Sasongko et al., 2007], was found in four new patients. In this study, the mutations p.R343X and p.R921X were newly detected in two patients, respectively. We have already presented a patient with p.R343X mutation [Ishihara et al., 2004], while p.R921X was previously reported in European patients [Zweier et al., 2005; Garavelli et al., 2009]. Five new mutations (i.e., p.Q271X, p.C312X, p.E609X, p.S800X, and p.S872X) have been identified in this study. In total, 13 kinds of nonsense mutations were found in 29 patients including three sibling cases (Table I). A total of

TABLE I. MWS Patients Associated With Nonsense *ZEB2* Mutations in the Japanese Population

No.	Case	Age	GD	EX	Mutation	Amino acid	ID	CFA	MC	CHD	S	HSCR	ACC/HCC	SP	Others	RF
1	S-073.a[a]	2 y 7 m	M	3	c.259G>T	p.E87X	++	+	−	−	+	−	−	−	−	[a]
2	S-073.b[a]	5 y 7 m	F	3	c.259G>T	p.E87X	++	+	−	−	+	−	−	−	−	[a]
3	S-073.c[a]	4 y 6 m	F	3	c.259G>T	p.E87X	++	+	−	−	+	−	ND	−	−	[a]
4	S-122	1 y 8 m	F	7	c.811C>T	p.Q271X	+	+	+	−	−	−	H	−	−	This study
5	S-031	7 y	M	7	c.904C>T	p.R302X	++	+	+	−	+	+	−	−	Cryptorchism	[b]
6	S-062	25 y	M	8	c.936C>A	p.C312X	++	+	+	ASD, PDA	+	+	A	B	Hypospadias, urinary disturbance, urethral stone	This study
7	S-014	4 y	M	8	c.1027C>T	p.R343X	++	+	+	ASD, PS	−	+	ND	−	Hypospadias	[b]
8	K-02	6 y	M	8	c.1027C>T	p.R343X	++	+	−	−	+	−, CO	−	−	Spinal bifida	This study
9	O-01	2 y	M	8	c.1027C>T	p.R343X	++	+	−	PDA	+	−, CO	H	−	Otitis media	This study
10	P-2[b]	8 y	F	8	c.1298C>T	p.Q433X	++	+	−	−	+	+	−	−	−	[c]
11	S-034	28 y	M	8	c.1489C>T	p.Q497X	++	+	−	−	+	−	ND	−	−	[b]
12	S-002	20 y	F	8	c.1645A>T	p.R549X	++	+	+	PDA	−	+	A	−	Exotropia	[d, b]
13	S-046	12 y 9 m	M	8	c.1825G>T	p.E609X	++	+	+	−	+	−, CO	H	−	−	This study
14	S-004	25 y	M	8	c.2083C>T	p.R695X	++	+	+	−	+	+	ND	−	HPS	[d, b]
15	S-006	28 y	M	8	c.2083C>T	p.R695X	++	+	+	−	+	−, CO	−	−	Exotropia	[b, e]
16	S-007	30 y	M	8	c.2083C>T	p.R695X	++	+	+	VSD	+	−, CO	−	−	Cryptorchism, esotropia	[b, e]
17	S-008	26 y	M	8	c.2083C>T	p.R695X	++	+	+	−	+	−, CO	−	−	−	[b, e]
18	S-021	6 y	M	8	c.2083C>T	p.R695X	++	+	+	PDA	+	+	ND	−	Hypospadias	[b]
19	S-032	2 y	M	8	c.2083C>T	p.R695X	++	+	−	PDA, VSD	+	+	H	−	Cryptorchism, hypospadias, HPS	[b]
20	S-038	3 y	F	8	c.2083C>T	p.R695X	++	+	+	PDA	+	+	−	−	Septum of vagina, exotropia	[b]
21	P-1[b]	5 y	F	8	c.2083C>T	p.R695X	++	+	+	PDA, VSD, AS, PS	+	−	−	−	Duplicated renal pelvis	[c]
22	S-097	14 y 8 m	F	8	c.2083C>T	p.R695X	++	+	−	−	−	−, CO	−	−	−	This study
23	S-112	10 y 9 m	M	8	c.2083C>T	p.R695X	++	+	+	PS	+	+	−	−	Hypospadias, otitis media, spleen hypoplasia	This study
24	S-118	3 y	M	8	c.2083C>T	p.R695X	++	+	−	−	−	−, CO	H	−	−	This study
25	S-120	2 y 11 m	M	8	c.2083C>T	p.R695X	++	+	+	ASD PS	+	−, CO	H	−	CWH, otitis media	This study
26	S-098	10 y	M	8	c.2399C>G	p.S800X	++	+	+	VSD PS	+	−	H	FW	Conduction deafness, exotropia	This study
27	S-054	8 y	F	8	c.2615C>G	p.S872X	++	+	+	−	+	−, CO	A	B	−	This study
28	S-101	6 y	M	8	c.2761C>T	p.R921X	++	+	+	VSD ASD	+	−	ND	B	Self-injury	This study
29	S-111	3 y 11 m	F	8	c.2761C>T	p.R921X	++	+	−	PDA	+	+, Short	−	−	−	This study

[a]The mutation was detected in three sibling patients [S-073.a–c] [a].
[b]P-1 and P-2 were reported as Patients 1 and 2, respectively [c].
GD, gender; EX, exon; ID, intellectual disability [++ severe, + moderate]; CFA, characteristic facial appearance; MC, microcephaly; CHD, congenital heart disease; S, seizures; HSCR, Hirschsprung disease; ACC/HCC, agenesis of the corpus callosum/hypoplasia of corpus callosum; SP, speech; RF, references; y, year; m, month; M, male; F, female; ND, not determined; ASD, atrial septal defect; PDA, patent ductus arteriosus; VSD, ventricular septal defect; AS, aortic stenosis; PS, pulmonary stenosis; CO, constipation; A, agenesis; H, hypoplasia; B, babbling; FW, few words; CWH, chordee without hypospadias; a, Ohtsuka et al. [2008]; b, Ishihara et al. [2004]; c, Sasongko et al. [2007]; d, Wakamatsu et al. [2001]; e, Yamada et al. [2001].

TABLE II. MWS Patients Associated With Frameshift *ZEB2* Mutations in the Japanese Population

No.	Case	Age	GD	EX	Mutation	Amino acid	ID	CFA	MC	CHD	S	HSCR	ACC/HCC	SP	Others	RF
1	S-108	7 y	M	3	c.[162_164]delC [CCC>CC]	p.P55Lfs*20	++	+	+	–	+	+	H	–	–	This study
2	S-128	5 y	M	3	c.[175_182]del5-bp [GAGACGAG>GAG]	p.T60Sfs*3	++	+	–	VSD	+	–	–	FW	Otitis media, hydronephrosis, self-injury	This study
3	S-010	6 y	F	3	c.[270_272]delG [GGG>GG]	p.G91Vfs*17	++	+	+	–	–	–	H	–	–	[b, e]
4	S-058	10 y	M	3	c.[311_312]dupA [AA>AA[A]]	p.A105Sfs*16	++	+	–	PDA	+	+	H	–	Hypospadias	This study
5	S-094	12 y 6 m	M	5	c.[459_460]delG [GG>G]	p.E154Rfs*58	++	+	+	PDA, AS, PS	–	+, Short	H	–	Bifid scrotum, blepharoptosis	This study
6	S-113	6 y	F	6	c.635_638dupCCTG [CCTG>CCTG[CCTG]]	p.P214Lfs*26	++	+	–	VSD	+	+	–	B	–	This study
7	S-115	5 y	F	6	c.647delG	p.C216Sfs*8	++	+	–	AS	–	+	H	–	–	This study
8	S-009	27 y	M	6	c.759_760dupCA [CA>CA [CA]]	p.Q255Pfs*8	++	+	+	–	+	–	–	–	–	[b, e]
9	S-047	15 y	M	7	c.[852_855]del2-bp [CACA>CA]	p.T285Rfs*9	++	+	+	ASD	+	+	H	–	Otitis media	This study
10	S-028	10 y	M	7	c.[855_858]del2-bp [AGAG>AG]	p.E286Vfs*8	++	+	+	PAS, PDA	+	–, CO	A	–	Cryptorchism	[b]
11	S131	1 y	M	7	c.[862_863]delG [GG>G]	p.G288Afs*10	ND	+	+	–	–	CO	A		Hypospadias	This study
12	S-015	5 y	M	8	c.1169ins382-bp [CAGGCCGGGE, 382-bp]	p.I390Tfs*41	++	+	+	–	+	–	H	–	–	[b]
13	S-076	11 y	F	8	c.[1169_1170]delT [TT>T]	p.T392Qfs*4	++	+	–	–	+	–	–	–	Exotropia	This study
14	S-005	25 y	M	8	c.[1174_1178]del4-bp [ACAGA>A]	p.T392Nfs*3	++	+	+	PDA	+	+	–	–	–	[d, b]
15	S-068	19 y	M	8	c.1176delG	p.E393Nfs*3	++	+	–	PDA, PS	+	+	–	–	HPS	This study
16	S-127	21 y	F	8	c.[1212_1213]delG [GG>G]	p.A405Lfs*12	++	+	–	PS	+	–, CO	–	FW	–	This study
17	S-103	6 y 2 m	F	8	c.[1268_1273]del4-bp [CCAGCC>CC]	p.S424Lfs*2	+	+	+	VSD	–	+	H	FW	AH	This study
18	S-050	18 y	M	8	c.1280_1286del7insACTGAG [GAGTTCA>ACTGAG]	p.G427Dfs*2	++	+	ND	–	ND	+, Long	ND	–	–	This study
19	S-102	8 y 10 m	F	8	c.[1334_1337]dupC [CCCC>CCCC[C]]	p.L447Ffs*9	++	+	+	ASD, PH, PS	+	–, CO	H	–	–	This study
20	S-024	11 y	F	8	c.1395_1408del14ins19 [GATTE,14-bp>CAAGE,19-bp]	p.Q465Hfs*9	++	+	+	PDA	+	+	–	–	–	[b]
21	S-090	8 y	F	8	c.1417delA	p.R473Gfs*14	++	+	+	–	+	–, CO	H	–	–	This study
22	K-01	8 y	F	8	c.1417delA	p.R473Gfs*14	++	+	+	–	+	–	–	–	Otitis media	This study
23	S-104	6 y 6 m	F	8	c.[1421_1426]dupA [AAAAAA>AAAAAA[A]]	p.M476Nfs*6	++	+	+	–	–	–, CO	–	–	Coloboma	This study
24	S-110	4 y 10 m	F	8	c.[1492_1493]delC [CC>C]	p.P498Lfs*18	++	+	–	PDA. T/F	+	–, CO	–	–	Duplicated renal pelvis	This study
25	S-066	12 y	F	8	c.[1534_1535]delG [GG>G]	p.G512Vfs*4	++	+	–	VSD	+	–, CO	–	FW	Hydronephrosis	This study
26	S-065	9 y	F	8	c.1822delG	p.E608Kfs*13	++	+	+	PDA	+	–, CO	–	–	–	This study
27	S-130	2 y 6 m	M	8	c.1966_1967delAT	p.M656Vfs*17	++	+	+	T/F	–	–, CO	–	–	HPS, high arched palate	This study
28	S-011	3 y	M	8	c.[2178_2180]delTT [TTT>T]	p.L727Ifs*28	++	+	+	–	+	–, CO	H	–	Exotropia	[b]

(*Continued*)

TABLE II. (Continued)

No.	Case	Age	GD	EX	Mutation	Amino acid	ID	CFA	MC	CHD	S	HSCR	ACC/HCC	SP	Others	RF
29	S-063	9 y	F	8	c.2254dupA [A>A[A]]	p.T752Nfs*4	++	+	+	T/F	+	+	A	B	Otitis media	This study
30	S-100	10 y 7 m	F	8	c. 2282delC	p.T761Kfs*26	++	+	–	PDA	+	–, CO	A	–	Otitis media	This study
31	S-106	12 y	F	8	c.[2349_2351]dupT [TT>TT[T]]	p.S784Ffs*11	++	+	+	–	+	–, CO	–	–	–	This study
32	S-049	23 y	M	8	c.2579delT	p.L860Rfs*3	++	+	+	–	+	+	H	–	Otitis media	This study
33	S-125	1 y 10 m	M	8	c.2740_2743dupCAGA [CAGAC>CAGA[CAGA]C]	p.S916Dfs*34	++	+	–	–	–	–	–	–	Cryptorchidism, hydronephrosis, intermittent exotropia	This study
34	S-121	1 y 10 m	M	10	c.[3608_3614]del5-bp [CAGACCA>CA]	p.D1204Rfs*29	++	+	–	PDA, VSD	+	–	H	–	Hypospadias	This study

EX, exon; ID, intellectual disability [++ severe, + moderate]; ND, not determined; CFA, characteristic facial appearance; MC, microcephaly; CHD, congenital heart disease; S, seizures; HSCR, Hirschsprung disease; ACC/HCC, agenesis of the corpus callosum/hypoplasia of corpus callosum; SP, speech; RF, references; y, year; m, month; M, male; F, female; ASD, atrial septal defect; PDA, patent ductus arteriosus; PAS, pulmonary artery sling; VSD, ventricular septal defect; AS, aortic stenosis; PH, pulmonary hypertension; PS, pulmonary stenosis; T/F, tetralogy of Fallot; CO, constipation; A, agenesis; H, hypoplasia; B, babbling; FW, few words; HPS, hypertrophic pyloric stenosis; AH, astigmatismus hypermetropicus; b, Ishihara et al. [2004]; d, Wakamatsu et al. [2001]; e, Yamada et al. [2001].

33 frameshift mutations from Japanese patients caused by small deletions, duplications, insertions, or other phenomena are summarized in Table II. In this study, 26 frameshift mutations were newly identified in 27 patients, and all the mutations were scattered between P55 and D1204. Only c.1417delA resulting in p.R473Hfs*14 was detected in two different patients. The mutations c.(852_855)del2-bp, c.(1421_1426)dupA, and c.2254dupA have been reported in European patients [Cacheux et al., 2001; Zweier et al., 2005; Garavelli et al., 2009]. Among the reported cases, the c.(3608_3614)del5-bp resulting in p.D1204Rfs*29 mutation is the closest to the C-terminal end.

Clinical Features in MWS Patients Associated With Nonsense and Frameshift Mutations

The clinical features of newly identified and previously reported Japanese patients with MWS harboring nonsense and frameshift mutations are summarized in Table III. All the patients showed severe to moderate intellectual disability and a characteristic facial appearance. It is noted that the sex ratio and most of the clinical features of these cases are quite similar to those in previous reports [Garavelli et al., 2009]. A detailed comparison of the results of this study with those from an earlier report showed that male/female ratio was 1.33 and 1.25, seizure frequencies were 78% and 74%, abnormalities of the corpus callosum were seen in 44% vs. 46%, and congenital heart disease was seen 54% and 54%, respectively. Five patients (S-066, S-098, S-103, S-127, and S-128) could speak a few words, and five patients (S-066, S-068, S-098, S-127, and S-128) could point at objects (e.g., food) kept out of reach. Characteristic facial appearance of seven patients is shown in Figure 1.

Instability of the ZEB2-D1204Rfs*29 Protein

The ZEB2-D1204Rfs*29 allele in S-121 encodes the longest 1,203 amino acid stretch from wild-type ZEB2 and an insertion of an additional 28 amino acids caused by a frameshift mutation at the C-terminus (total 1,231 amino acids). The molecular mass of FLAG-tagged wild-type ZEB2 and ZEB2-D1204Rfs*29 were calculated to be 139.7 and 141.9 kDa, respectively. To characterize the mutant ZEB2, we examined the mRNA levels of the transiently expressed wild-type and mutant ZEB2 by multiplex PCR, but no marked differences were observed (Fig. 2B). Next, we performed Western blotting in the cells. The results demonstrated that the ZEB2 protein level in cells harboring the p.D1204Rfs*29 mutation is remarkably decreased compared to that of the wild-type-expressing cells. In contrast, the ZEB2 protein levels in cells harboring the p.D1204X or p.M1210X mutants were not decreased. Moreover, the expression of ZEB2-D1204Rfs*29 was approximately 20% that of the wild-type (Fig. 2B) and the difference in the molecular mass of ZEB2-D1204Rfs*29 and wild-type ZEB2 was found to be more than 10 kDa (Fig. 2C). This is larger than the calculated MW difference of the two proteins, which is 2.2 kDa.

DISCUSSION

To date, more and more pediatricians, pediatric neurologists, pediatric surgeons, human geneticists, and genetic counselors in

TABLE III. Clinical Features of MWS Patients Associated With Nonsense and Frameshift Mutations

	Nonsense mutations, Table I [A]		Frameshift mutations, Table II [B]		
	This study (n = 13)	Total (n = 29)	This study (n = 27)	Total (n = 34)	[A] + [B] (n = 63)
Male/female	9/4	19/10	12/15	17/17	36/27
Intellectual disability	All	All	All	All	All
Microcephaly	8/13 (62%)	18/29 (62%)	14/27 (52%)	21/34 (62%)	39/63 (62%)
Seizures	10/13 (77%)	24/29 (83%)	19/27 (70%)	25/34 (74%)	49/63 (78%)
Hypoplasia or agenesis of the corpus callosum	9/13 (69%)	11/29 (38%)	13/27 (48%)	17/34 (50%)	28/63 (44%)
Congenital heart disease	7/13 (54%)	14/29 (48%)	17/27 (63%)	20/34 (59%)	34/63 (54%)
Hirschsprung disease	3/13 (23%)	11/29 (38%)	11/27 (41%)	13/34 (38%)	24/63 (38%)
Constipation	7/13 (54%)	10/29 (35%)	11/27 (41%)	13/34 (38%)	23/63 (37%)
Urogenital/renal anomalies	3/13 (23%)	10/29 (35%)	8/27 (30%)	9/34 (26%)	19/63 (30%)

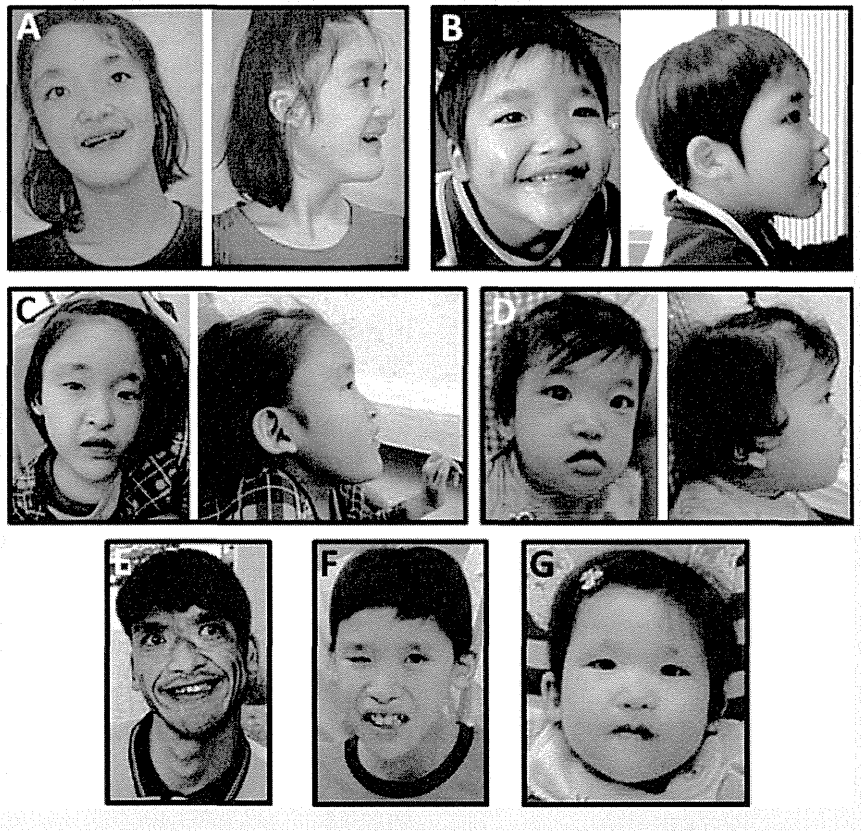

FIG. 1. Facial appearance of MWS patients. A: S-97 (12-year-2-month-old female). B: S-98 (4-year-10-month-old male). C: S-100 (7-year-2-month-old female). D: S-110 (1-year-8-month-old male). E: S-8 (36-year-old male). F: S-94 (10-year-5-month-old male). G: S-111 (1-year-10-month-old female). The patients have eyebrows with medially flaring and sparse in the lateral, large and deep-set eyes, telecanthus, broad nasal bridge, depressed nasal bridge, prominent and triangular chin, and uplifted ear lobes. Smiling face (A, B, E, F), thin chestnut hair (B–D, G), frontal bossing (B–D, G), hypertelorism (A–E), round nasal tip with a prominent columella and a short philtrum (A–F) and posteriorly rotated ears (A, B, D) are also noted. S94 (F) has right ptosis.

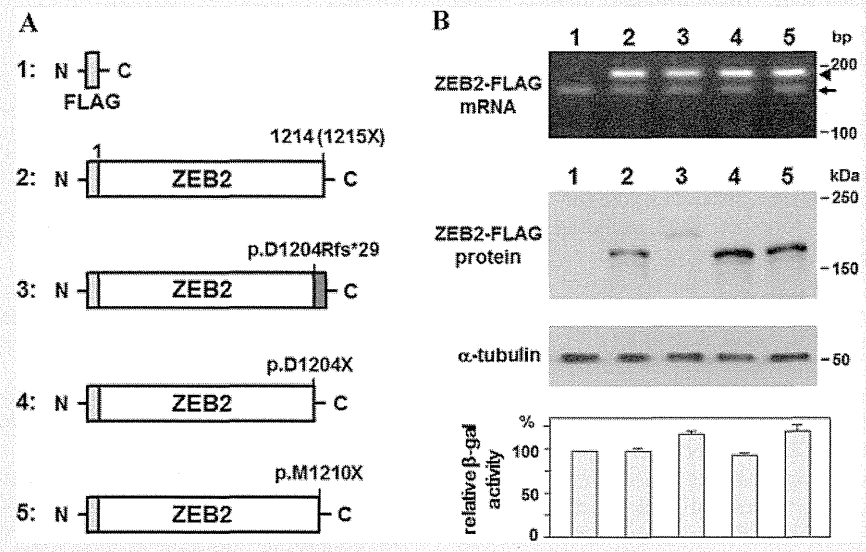

FIG. 2. Expression of wild-type and mutant ZEB2 proteins in HEK293 cells. A: A schematic illustration of FLAG-tagged ZEB2 mutants. B: First (topmost) panel. Multiplex PCR analysis of the FLAG tagged ZEB2 mRNA levels relative to ACTB in HEK293 cells transfected with each of the ZEB2-expressing vectors. Arrow and arrowhead indicated the PCR products of ACTB and FLAG tagged ZEB2, respectively. Second and third panels: Western blot analysis of HEK293 cells transfected with each of the ZEB2-expressing vectors using antibodies specific for FLAG and α-tubulin. Fourth panel: relative *E. coli* β-galactosidase (β-gal) activities in each transfected group of HEK293 cells. The vertical bars indicate the standard error of the mean for three experiments. Lane 1, pFLAG vector; lane 2, wild-type pFLAG-ZEB2; lane 3, pFLAG-ZEB2-D1204Rfs*29; lane 4, pFLAG-ZEB2-D1204X; lane 5, pFLAG-ZEB2-M1210X.

Japan recognize MWS based on the characteristic facial appearance and moderate or severe intellectual disability, similar to that seen in Down syndrome. There is no obvious genotype–phenotype correlation in the MWS patients except for large deletions (>10 Mb) at the 2q22-24 locus [Zweier et al., 2003; Ishihara et al., 2004]; yet we speculate that clinical features of MWS may become rather unclear when we include the deletion types harboring wide clinical symptoms. Thus, we have focused on the clinical features of MWS caused by nonsense and frameshift mutations in *ZEB2* in this study. We have identified 13 nonsense and 27 frameshift *ZEB2* mutations in 40 newly identified MWS patients. Thus, the overall number of nonsense and frameshift mutations of the so far identified Japanese MWS patients are 29 and 34, respectively, including those from previous studies [Yamada et al., 2001; Ishihara et al., 2004; Sasongko et al., 2007; Ohtsuka et al., 2008]. All the patients have the characteristic facial appearance, and moderate or severe intellectual disability. Compared to previous reports of the clinical summary of MWS including deletion cases [Dastot-Le Moal et al., 2007], the frequencies of patients showing seizures, abnormalities of corpus callosum, or congenital heart disease are quite similar; however, the frequencies of microcephaly (62% vs. 80%), Hirschsprung disease (38% vs. 54%), and urogenital/renal anomalies (30% vs. 52%) are lower than those previously reported (Table III) [Garavelli et al., 2009]. We observed that microcephaly is evident at a later age in some patients. For example: (1) S-090, occipitofrontal circumference (OFC): −1.0 standard deviation (SD) (at birth) and −2.5 SD (3 years old), (2) S-106, OFC: 0 SD (at birth) and −2 SD (9 years old) with failure to thrive. Thus, microcephaly may not be characteristic of the younger patients (~6 years old) in this study. Further case studies are necessary to investigate whether nonsense and frameshift mutations in *ZEB2* are responsible for the relatively lower number of Hirschsprung disease and urogenital/renal anomalies in this study. In addition, the urethral stones (S-062), spleen hypoplasia (S-112), chordee without hypospadias (S-120), duplicated renal pelvis (S-110 and P-1), and spinal bifida (K-02) identified in this study are rare in MWS. Further case studies are also necessary to establish whether these are symptoms associated with MWS. We found that two patients (S-101 and S-128) have self-injuries, in accordance with a recent study showing that MWS was associated with significant levels of behavioral and emotional problems [Evans et al., 2012].

In this study, using transient transfection, we demonstrated that the ZEB2-D1204Rfs*29 protein has a larger mass, but its protein level was remarkably decreased without a remarkable change in the mRNA level when compared to that of the wild-type ZEB2. Thus, MWS was caused by the ZEB2 protein instability in S-121. The D1204Rfs*29 mutation generates a new terminal codon. Consequently, the 11 C-terminal amino acid sequence (DHEEDNMEDGM) encoded by wild-type ZEB2 was replaced by a 28-amino acid sequence (RGRQYGRWHVNYCILSFHFFFPVVLLPA) by the frameshift mutation. Comparing the two C-terminal peptides, 6 (underlined) out of 11 amino acids were negatively charged

amino acids, while 15 (double underlined) out of 28 amino acids were hydrophobic amino acids. This remarkably different amino acid composition suggests that conformation of the C-termini of the two ZEB2 proteins would differ. Secondary structure analysis of the C-terminus of the wild-type and D1204Rfs*29 proteins using "Jpred consensus method for protein secondary structure prediction server" indicated a dramatically increased potential for alpha helix formation with strong hydrophobicity in the C-terminal peptide of ZEB2-D1204Rfs*29 [Cole et al., 2008]. This could affect the post-translational modifications of mutant ZEB2, including processing, phosphorylation, or glycosylation as well as protein stability, which could explain the Western blot findings. A different C-terminal frameshift mutation in ZEB2 has been reported in MWS where the c.3567-3568insCC frameshift mutation (causing a 2-bp insertion) produces a longer ZEB2 (p.M1190Pfs*50) than ZEB2-D1204Rfs*29; however, the characterization of the mutant ZEB2 has not been performed. The finding that nonsense mutations (1204X and 1210X) at the C-terminus of ZEB2 do not affect the protein stability suggests that these mutations may not cause typical MWS. To confirm these hypotheses, C-terminal analysis of the mutant ZEB2, case studies of MWS with C-terminus mutations, or single nucleotide polymorphism analyses of normal populations are necessary.

ACKNOWLEDGMENTS

We are grateful to the patients and their families for agreeing to participate in this study. Epidemiological survey was conducted by S.M. and K.K. This study was supported by the Takeda Science Foundation and a Health Labor Sciences Research Grant (to N.W.).

REFERENCES

Cacheux V, Dastot-Le Moal F, Kääriäinen H, Bondurand N, Rintala R, Boissier B, Wilson M, Mowat D, Goossens M. 2001. Loss-of-function mutations in *SIP1* Smad interacting protein 1 result in a syndromic Hirschsprung disease. Hum Mol Genet 10:1503–1510.

Cecconi M, Forzano F, Garavelli L, Pantaleoni C, Grasso M, Dagna Bricarelli F, Perroni L, Di Maria E, Faravelli F. 2008. Recurrence of Mowat–Wilson syndrome in siblings with a novel mutation in the *ZEB2* gene. Am J Med Genet Part A 146A:3095–3099.

Cole C, Barber JD, Barton GJ. 2008. The Jpred 3 secondary structure prediction server. Nucleic Acids Res 36:W197–W201.

Dastot-Le Moal F, Wilson M, Mowat D, Collot N, Niel F, Goossens M. 2007. *ZFHX1B* mutations in patients with Mowat–Wilson syndrome. Hum Mutat 28:313–321.

Evans E, Einfeld S, Mowat D, Taffe J, Tonge B, Wilson M. 2012. The behavioral phenotype of Mowat–Wilson syndrome. Am J Med Genet Part A 158A:358–366.

Garavelli L, Zollino M, Mainardi PC, Gurrieri F, Rivieri F, Soli F, Verri R, Albertini E, Favaron E, Zignani M, Orteschi D, Bianchi P, Faravelli F, Forzano F, Seri M, Wischmeijer A, Turchetti D, Pompilii E, Gnoli M, Cocchi G, Mazzanti L, Bergamaschi R, De Brasi D, Sperandeo MP, Mari F, Uliana V, Mostardini R, Cecconi M, Grasso M, Sassi S, Sebastio G, Renieri A, Silengo M, Bernasconi S, Wakamatsu N, Neri G. 2009. Mowat–Wilson syndrome: Facial phenotype changing with age: Study of 19 Italian patients and review of the literature. Am J Med Genet Part A 149A: 417–426.

Ishihara N, Yamada K, Yamada Y, Miura K, Kato J, Kuwabara N, Hara Y, Kobayashi Y, Hoshino K, Nomura Y, Mimaki M, Ohya K, Matsushima M, Nitta H, Tanaka K, Segawa M, Ohki T, Ezoe T, Kumagai T, Onuma A, Kuroda T, Yoneda M, Yamanaka T, Saeki M, Segawa M, Saji T, Nagaya M, Wakamatsu N. 2004. Clinical and molecular analysis of Mowat–Wilson syndrome associated with *ZFHX1B* mutations and deletions at 2q22-q24.1. J Med Genet 41:387–393.

Lurie IW, Supovitz KR, Rosenblum-Vos LS, Wulfsberg EA. 1994. Phenotypic variability of del(2)(q22-q23): Report of a case with a review of the literature. Genet Couns 5:11–14.

McGaughran J, Sinnott S, Dastot-Le Moal F, Wilson M, Mowat D, Sutton B, Goossens M. 2005. Recurrence of Mowat-Wilson syndrome in siblings with the same proven mutation. Am J Med Genet A 137A:302–304.

McKinsey GL, Lindtner S, Trzcinski B, Visel A, Pennacchio LA, Huylebroeck D, Higashi Y, Rubenstein JL. 2013. *Dlx1&2*-dependent expression of *Zfhx1b* (*Sip1*, *Zeb2*) regulates the fate switch between cortical and striatal interneurons. Neuron 77:83–98.

Mowat DR, Croaker GD, Cass DT, Kerr BA, Chaitow J, Adès LC, Chia NL, Wilson MJ. 1998. Hirschsprung disease, microcephaly, mental retardation, and characteristic facial features: Delineation of a new syndrome and identification of a locus at chromosome 2q22-q23. J Med Genet 35:617–623.

Mowat DR, Wilson MJ, Goossens M. 2003. Mowat–Wilson syndrome. J Med Genet 40:305–310.

Ohtsuka M, Oguni H, Ito Y, Nakayama T, Matsuo M, Osawa M, Saito K, Yamada Y, Wakamatsu N. 2008. Mowat–Wilson syndrome affecting 3 siblings. J Child Neurol 23:274–278.

Postigo AA, Depp JL, Taylor JJ, Kroll KL. 2003. Regulation of Smad signaling through a differential recruitment of coactivators and corepressors by ZEB proteins. EMBO J 22:2453–2462.

Sasongko TH, Sadewa AH, Gunadi Lee MJ, Koterazawa K, Nishio H. 2007. Nonsense mutations of the *ZFHX1B* gene in two Japanese girls with Mowat–Wilson syndrome. Kobe J Med Sci 53:157–162.

Seuntjens E, Nityanandam A, Miquelajauregui A, Debruyn J, Stryjewska A, Goebbels S, Nave KA, Huylebroeck D, Tarabykin V. 2009. Sip1 regulates sequential fate decisions by feedback signaling from postmitotic neurons to progenitors. Nat Neurosci 12:1373–1380.

Verschueren K, Remacle JE, Collart C, Kraft H, Baker BS, Tylzanowski P, Nelles L, Wuytens G, Su MT, Bodmer R, Smith JC, Huylebroeck D. 1999. SIP1, a novel zinc finger/homeodomain repressor, interacts with Smad proteins and binds to 5′-CACCT sequences in candidate target genes. J Biol Chem 274:20489–20498.

Verstappen G, van Grunsven LA, Michiels C, Van de Putte T, Souopgui J, Van Damme J, Bellefroid E, Vandekerckhove J, Huylebroeck D. 2008. Atypical Mowat–Wilson patient confirms the importance of the novel association between ZFHX1B/SIP1 and NuRD corepressor complex. Hum Mol Genet 17:1175–1183.

Wakamatsu N, Yamada Y, Yamada K, Ono T, Nomura N, Taniguchi H, Kitoh H, Mutoh N, Yamanaka T, Mushiake K, Kato K, Sonta S, Nagaya M. 2001. Mutations in *SIP1*, encoding Smad interacting protein-1, cause a form of Hirschsprung disease. Nat Genet 27:369–370.

Weng Q, Chen Y, Wang H, Xu X, Yang B, He Q, Shou W, Chen Y, Higashi Y, van den Berghe V, Seuntjens E, Kernie SG, Bukshpun P, Sherr EH, Huylebroeck D, Lu QR. 2012. Dual-mode modulation of Smad signaling by Smad-interacting protein Sip1 is required for myelination in the central nervous system. Neuron 73:713–728.

Yamada K, Yamada Y, Nomura N, Miura K, Wakako R, Hayakawa C, Matsumoto A, Kumagai T, Yoshimura I, Miyazaki S, Kato K, Sonta S,

Ono H, Yamanaka T, Nagaya M, Wakamatsu N. 2001. Nonsense and frameshift mutations in *ZFHX1B*, encoding Smad-interacting protein 1, cause a complex developmental disorder with a great variety of clinical features. Am J Hum Genet 69:1178–1185.

Yamada K, Takado Y, Kato YS, Yamada Y, Ishiguro H, Wakamatsu N. 2013. Characterization of the mutant β-subunit of β-hexosaminidase for dimer formation responsible for the adult form of Sandhoff disease with the motor neuron disease phenotype. J Biochem 153:111–119.

Zweier C, Albrecht B, Mitulla B, Behrens R, Beese M, Gillessen-Kaesbach G, Rott HD, Rauch A. 2002. "Mowat–Wilson" syndrome with and without Hirschsprung disease is a distinct, recognizable multiple congenital anomalies-mental retardation syndrome caused by mutations in the zinc finger homeobox 1B gene. Am J Med Genet 108:177–181.

Zweier C, Temple IK, Beemer F, Zackai E, Lerman-Sagie T, Weschke B, Anderson CE, Rauch A. 2003. Characterisation of deletions of the *ZFHX1B* region and genotype–phenotype analysis in Mowat–Wilson syndrome. J Med Genet 40:601–605.

Zweier C, Thiel CT, Dufke A, Crow YJ, Meinecke P, Suri M, Ala-Mello S, Beemer F, Bernasconi S, Bianchi P, Bier A, Devriendt K, Dimitrov B, Firth H, Gallagher RC, Garavelli L, Gillessen-Kaesbach G, Hudgins L, Kääriäinen H, Karstens S, Krantz I, Mannhardt A, Medne L, Mücke J, Kibaek M, Krogh LN, Peippo M, Rittinger O, Schulz S, Schelley SL, Temple IK, Dennis NR, Van der Knaap MS, Wheeler P, Yerushalmi B, Zenker M, Seidel H, Lachmeijer A, Prescott T, Kraus C, Lowry RB, Rauch A. 2005. Clinical and mutational spectrum of Mowat–Wilson syndrome. Eur J Med Genet 48:97–111.

CLINICAL GENETICS An International Journal of Genetics, Molecular and Personalized Medicine

Clin Genet 2014
Printed in Singapore. All rights reserved

CLINICAL GENETICS
doi: 10.1111/cge.12496

Short Report

Autosomal recessive cystinuria caused by genome-wide paternal uniparental isodisomy in a patient with Beckwith–Wiedemann syndrome

Ohtsuka Y, Higashimoto K, Sasaki K, Jozaki K, Yoshinaga H, Okamoto N, Takama Y, Kubota A, Nakayama M, Yatsuki H, Nishioka K, Joh K, Mukai T, Yoshiura K-i, Soejima H. Autosomal recessive cystinuria caused by genome-wide paternal uniparental isodisomy in a patient with Beckwith–Wiedemann syndrome.
Clin Genet 2014. © John Wiley & Sons A/S. Published by John Wiley & Sons Ltd, 2014

Approximately 20% of Beckwith–Wiedemann syndrome (BWS) cases are caused by mosaic paternal uniparental disomy of chromosome 11 (pUPD11). Although pUPD11 is usually limited to the short arm of chromosome 11, a small minority of BWS cases show genome-wide mosaic pUPD (GWpUPD). These patients show variable clinical features depending on mosaic ratio, imprinting status of other chromosomes, and paternally inherited recessive mutations. To date, there have been no reports of a mosaic GWpUPD patient with an autosomal recessive disease caused by a paternally inherited recessive mutation. Here, we describe a patient concurrently showing the clinical features of BWS and autosomal recessive cystinuria. Genetic analyses revealed that the patient has mosaic GWpUPD and an inherited paternal homozygous mutation in *SLC7A9*. This is the first report indicating that a paternally inherited recessive mutation can cause an autosomal recessive disease in cases of GWpUPD mosaicism. Investigation into recessive mutations and the dysregulation of imprinting domains is critical in understanding precise clinical conditions of patients with mosaic GWpUPD.

Conflict of interest

The authors have no competing financial interests to declare.

Y. Ohtsuka[a], K. Higashimoto[a], K. Sasaki[b], K. Jozaki[a], H. Yoshinaga[a], N. Okamoto[c], Y. Takama[d], A. Kubota[d], M. Nakayama[e], H. Yatsuki[a], K. Nishioka[a], K. Joh[a], T. Mukai[f], K.-i. Yoshiura[b] and H. Soejima[a]

[a]Division of Molecular Genetics and Epigenetics, Department of Biomolecular Sciences, Faculty of Medicine, Saga University, Saga, Japan, [b]Department of Human Genetics, Nagasaki University Graduate School of Biomedical Sciences, Nagasaki, Japan, [c]Department of Medical Genetics , [d]Department of Pediatric Surgery , [e]Department of Pathology, Osaka Medical Center and Research Institute for Maternal and Child Health, Osaka, Japan, and [f]Nishikyushu University, Saga, Japan

Key words: Beckwith–Wiedemann syndrome – cystinuria – genome-wide paternal uniparental disomy mosaicism – *SLC3A1* – *SLC7A9*

Corresponding author: Hidenobu Soejima, Division of Molecular Genetics and Epigenetics, Department of Biomolecular Sciences, Faculty of Medicine, Saga University, 5-1-1 Nabeshima, Saga 849-8501, Japan.
Tel.: +81 952 34 2260;
fax: +81 952 34 2067;
e-mail: soejimah@med.saga-u.ac.jp

Received 8 July 2014, revised and accepted for publication 27 August 2014

Beckwith–Wiedemann syndrome (BWS) (OMIM #130650) is an imprinting disorder characterized by peculiar prenatal and postnatal macrosomia, macroglossia, and abdominal wall defects. There are various genetic and epigenetic abnormalities that can cause BWS, although paternal uniparental disomy of 11p15 (pUPD11) accounts for around 20% of cases (1, 2). The minimum pUPD size is approximately 2.7 Mb from

the telomere of 11p, including both imprinting control regions, *H19*DMR and *Kv*DMR1 (3). pUPD11 causes hypermethylation of *H19*DMR and hypomethylation of *Kv*DMR1, which leads to overexpression of *IGF2* and reduced expression of *H19* and *CDKN1C*. In its most wide-reaching variety, pUPD acts on the whole genome, and is denoted as genome-wide pUPD (GWpUPD). Non-mosaic GWpUPD results in the formation of a hydatidiform mole, while individuals with GWpUPD mosaicism are born alive (2). GWpUPD patients usually show clinical features of BWS and other variable features thought to depend on the mosaic ratio, the imprinting status of other chromosomes such as chromosomes 6, 14, 15, and 20 (pUPDs of these chromosomes cause other imprinting disorders), and paternally inherited recessive mutations (4). However, to date, there have been no reports of a mosaic GWpUPD patient with an autosomal recessive disease caused by a paternally inherited recessive mutation.

Cystinuria (OMIM #220100) is an autosomal recessive disorder characterized by impaired epithelial cell transport of cystine and dibasic amino acids (lysine, ornithine, and arginine) in the proximal renal tubule and gastrointestinal tract. The impaired renal reabsorption and the low solubility of cystine cause the formation of calculi in the urinary tract (5). Causative genes for cystinuria include *SLC3A1* and *SLC7A9*. These genes encode proteins that comprise the rBAT/$b^{0,+}$AT heterodimer, which mediates the exchange of extracellular cationic amino acids and cystine for intracellular neutral amino acids (6).

We investigated a patient with clinical features of both BWS and cystinuria. Genetic analyses revealed that the patient harbored mosaic GWpUPD and inherited a homozygous mutation of *SLC7A9* paternally. This is the first reported case of a patient with these features exhibited concurrently.

Materials and methods

Patient report

The female infant with a karyotype of 46,XX was the first-born baby to non-consanguineous, healthy, Japanese parents after 34 weeks and 6 days of gestation. Her birth weight was 4254 g [+6.8 SD (standard deviation)], and she exhibited omphalocele, macroglossia, and nevus flammeus on her forehead. These conditions satisfy the diagnostic criteria for BWS as described by Weksberg et al. (7). After birth, she also manifested persistent hyperinsulinemic hypoglycemia and an extremely high level of serum alpha-fetoprotein (300,000 ng/ml). She was diagnosed with diffuse nesidioblastosis in the pancreatic body, and a partial pancreatectomy was performed twice, at 2 months and at 8 years of age (8). In addition, at puberty she had bilateral breast fibroadenomas and an ovarian adenofibroma, as recently reported (9). She did not develop any mental or motor delay.

Atrophy of the left kidney and enlargement of the right kidney were detected at birth, and urinary stones in the bladder and medullary calcinosis in both kidneys were detected at 10 months of age (Fig. 1). The

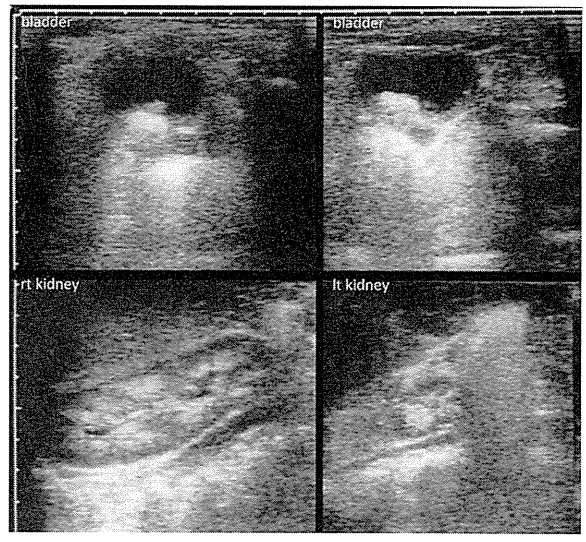

Fig. 1. Sonography of urolithiasis. Ultrasound images of the patient at one year of age shows a 1 cm stone in the bladder and medullary calcinosis in both kidneys. Atrophy of the left kidney was diagnosed at birth.

urinary amino acid analysis revealed high concentrations of cystine (551 μmol/l), lysine (5175 μmol/l), and arginine (3837 μmol/l), and cystine crystals were visible in a urine sample. Therefore, she was also diagnosed with cystinuria. Her parents had no history of urolithiasis; however, cystine and lysine in the father's urine were moderately elevated (296 μmol/l and 850 μmol/l, respectively).

This study was approved by the Ethics Committee for Human Genome and Gene Analyses of the Faculty of Medicine, Saga University.

DNA isolation

Genomic DNA was extracted from the peripheral blood of the patient and her parents, the patient's pancreas, and urine using commercially available DNA extraction kits.

SNP array analysis

Single nucleotide polymorphism (SNP) array analysis was performed with Genome-Wide Human SNP Array 5.0 (Affymetrix, Santa Clara, CA) according to the manufacturer's protocol. The genotype was analyzed using GENOTYPING CONSOLE (GTC) 4.1 software (Affymetrix). Copy number, allele ratio, and trio SNP analyses were performed using PARTEK GENOMICS SUITE version 6.6 beta (Partek Inc., St. Louis, MO). A reference generated from 89 Japanese samples was used. The genomic positions of the SNPs corresponded to GRCh37/hg19.

Mutation analyses of *SLC3A1* and *SLC7A9* genes

All coding exons and flanking intronic regions of *SLC3A1* and *SLC7A9* genes were amplified by polymerase chain reaction (PCR) and directly sequenced.

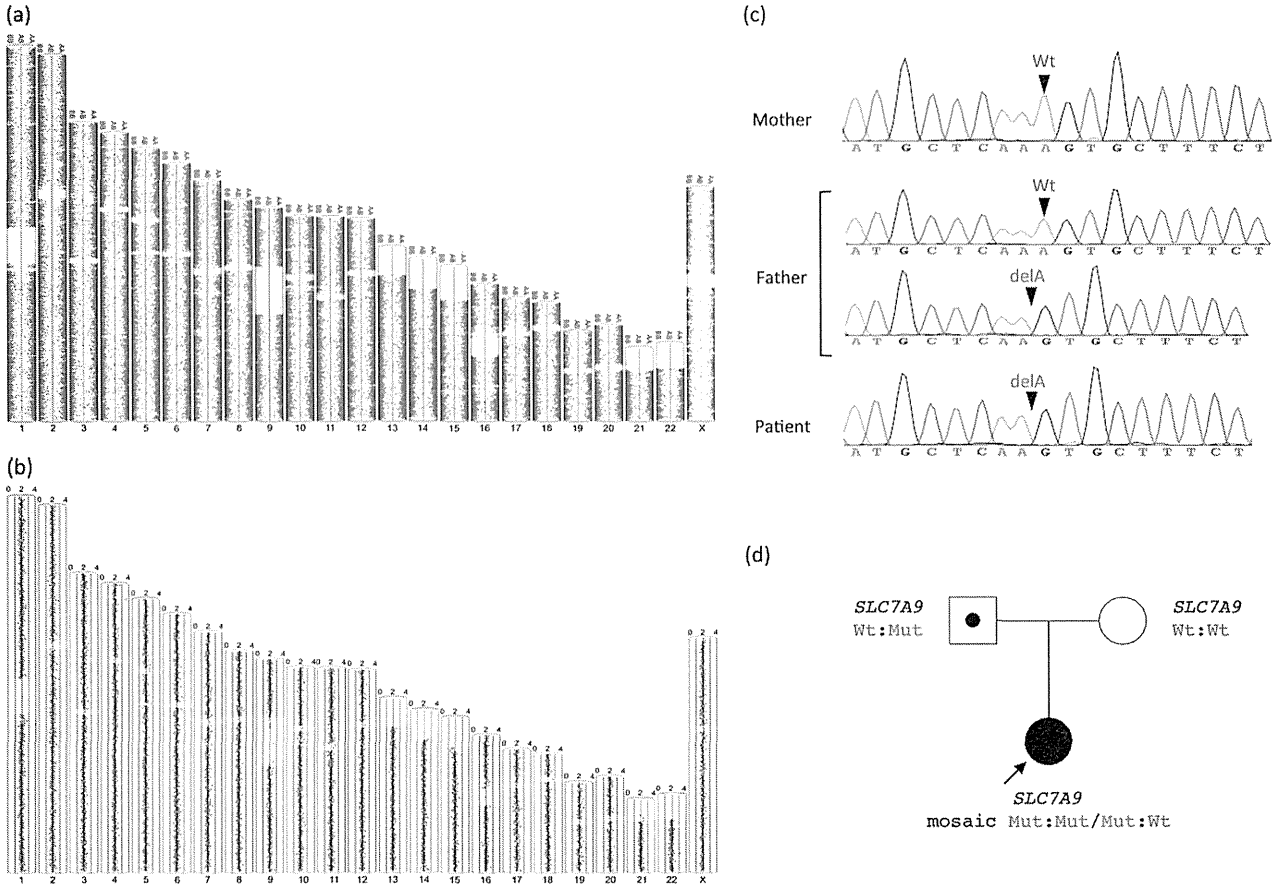

Fig. 2. Results of single nucleotide polymorphism (SNP) array analysis and mutation analysis of a cystinuria causative gene, *SLC7A9*. (**a**, **b**) Results of patient SNP array analysis. Genotyping (**a**) showed homozygous (AA or BB) results for almost all SNPs throughout all chromosomes, and absence of aberrant copy number variation (**b**); this evidence supports the notion of mosaicism for genome-wide paternal uniparental disomy (GWpUPD) of isodisomic androgenetic cells and normal biparental cells. (**c**) Results of mutation analysis of a cystinuria causative gene, *SLC7A9*. Sanger sequencing revealed a single-base deletion in exon 10 in both the father and the patient. Polymerase chain reaction (PCR)-cloning-sequencing revealed four wild-type clones and nine mutant clones in the father, indicating heterozygosity for the mutation. PCR direct sequencing showed that the patient seemed to be homozygous for the mutation because of a high mosaic ratio for GWpUPD. The mother did not have the mutation. (**d**) Patient's family pedigree. The *SLC7A9* mutation found in the patient was paternally inherited. In the patient, cells with GWpUPD were homozygous for the mutation, whereas biparental cells were heterozygous, containing both the mutation and the maternally inherited wild-type allele.

The PCR product of *SLC7A9* exon 10 in the father was cloned into a pT7Blue T-Vector (Novagen, San Diego, CA), and individual clones were sequenced. Primers for the mutation analyses are listed in Table S1, Supporting Information.

Results

To identify the potential cause of the BWS, we first performed methylation-sensitive Southern blots of two imprinting control regions at 11p15, *H19*DMR, and *Kv*DMR1. The methylation index (MI) was 99% at *H19*DMR and 2% at *Kv*DMR1 (Fig. S1). Because *H19*DMR is methylated on the paternal allele and *Kv*DMR1 is methylated on the maternal allele, pUPD of the region with a high mosaic ratio was strongly suggested.

We then performed microarray analysis of the patient, father, and mother SNP trios using SNP Array 5.0. The results showed two normal copies in the patient and her parents; however, the patient's genotype contained homozygous (AA or BB) results for almost all SNPs throughout all chromosomes (Fig. 2a,b). The genotyping of the trios indicated that the informative SNPs in the patient had been transmitted via paternal uniparental inheritance (data of chromosomes 2 and 19 are shown in Fig. S2). To calculate the mosaic ratio, we quantitatively analyzed microsatellite markers across all chromosomes except chromosome Y. In the patient, the average mosaic ratio of all informative markers was 91% in the peripheral blood and 83% in the pancreas (Table S2). These results indicated GWpUPD mosaicism of isodisomic androgenetic cells and normal biparental cells. Because mosaic GWpUPD necessarily includes 11p15.4-p15.5, we concluded that the causative abnormality for the BWS phenotype was pUPD11.

Finally, because the patient was diagnosed with autosomal recessive cystinuria, we performed mutation analyses of the supposed causative genes for cystinuria, *SLC3A1* at 2p21 and *SLC7A9* at 19q13.1. The

Table 1. Literature review of live-born patients with genome-wide paternal UPD[a]

	Our patient	Johnson et al. (13)	Kalish et al. (12)			Gogiel et al. (15)	Inbar-Feigenberg et al. (14)	Yamazawa et al. (4)	Romanelli et al. (16)	Wilson et al. (17)		Reed et al. (18)	Giurgea et al. (19)	Bryke and Garber (20)	Hoban et al. (21)
			Patient #1	Patient #2	Patient #3					Patient #1	Patient #2				
Gestational age	34 weeks 6 days	30 weeks 6 days	31 weeks 5 days	30 weeks 6 days	24 weeks 1 days	37 weeks	33 weeks	34 weeks		36 weeks	29 weeks 6 days	30 weeks 4 days	35 weeks		42 weeks
Birth weight (g)	4254	2460				3850	2270	3730	3750			1110	2260		
Weight percentile	>97th	>97th	85th	95th	50th	>90th	75th	>97th		>97th	>90th		25–50th		
Macroglossia	+			+		+		+		+					
Abdominal wall defect	+	+	+	+	+	+	+	+		+	+				
Visceromegaly	+		+	+	+	+	+	+		+	+			+	
Hemihyperplasia		+	+	+		+	+	+	+		+		+	+	+
Hypoglycemia	+	+	+	+	+	+	+	+	+	+	+		+		
Cutaneous abnormality	+		+	+			+		+		+			+	
Cardiac abnormality	+		+			+	+			+				+	
Neurological abnormality			+				+	+	+	+	+			+	
Tumor development	+		+	+	+	+	+	+	+	+	+	+	+	+	+
Failure to thrive				+				+		+	+			+	
Placental abnormality	+		+	+		+	+	+			+	+			
Other abnormality			+	+	+	+	+	+	+	+	+			+	
Features estimated paternal UPD	UPD11	UPD11	UPD11, 14	UPD11	UPD11	UPD11, 14	UPD11, 15, 20	UPD11, 14, 15	UPD11, 15	UPD11	UPD11		UPD11	UPD6, 14, 15, 20	UPD11
Other findings	Cystinuria (homozygous mutation of *SLC7A9*)	Hyperkalemia, abdominal swelling, deceased		Peripheral pulmonic stenosis, small bowel obstructions	Respiratory distress, cliteromegaly, deceased	Cerebral seizure, non-obliterating thrombosis of the inferior vena cava, multiple fractures, tachypnea	Strabismus, renal dysplasia, respiratory distress, small choroid plexus bleed, low level of 25-hydroxy vitamin D	Asphyxia	Renal stone	Respiratory insufficiency, inflammatory condition, granulocyte hyperplasia, arthritis, stenosis of arteries, hemiplegic stroke, hypertension		Fetal distress			

UPD, uniparental disomy.

[a]Cutaneous abnormality: hemangioma, cutaneous capillary vascular malformation or pigmentation. Neurological abnormality: developmental and motor delay, hypotonia, convulsion or autism. Other abnormality: ear lobe anomaly, hypertelorism, abnormal facies, bell-shaped thorax, or others.

SNP array showed two normal copies of both regions (Fig. S2). Sanger sequencing revealed a single-base deletion in exon 10 of *SLC7A9*, which led to a previously reported frameshift mutation (c.1017delA, p.V340fsX21, RefSeq: NM_001126335) (10), whereas no mutation was found in *SLC3A1* (Fig. 2c). The father was a heterozygous carrier of the mutation showing moderately elevated cystine and lysine in his urine without urolithiasis, while the mother was homozygous for the wild-type allele (Fig. 2c). The patient seemed to be homozygous for the mutation because of the high mosaic ratio of GWpUPD (Fig. 2c,d). *In silico* prediction programs such as MutationTaster (http://www.mutationtaster.org/) and SIFT-indels (http://sift.bii.a-star.edu.sg/www/SIFT_indels2.html) predicted the *SLC7A9* mutation as 'DISEASE CAUSING' and 'DAMAGING', respectively. The mutation could not be found after a comprehensive database search covering dbSNP (http://www.ncbi.nlm.nih.gov/projects/SNP/), 1000 Genomes (http://www.1000genomes.org/), ClinVar (http://www.ncbi.nlm.nih.gov/clinvar/), the Human Genome Variation Database (http://www.genome.med.kyoto-u.ac.jp/SnpDB/index.html), and the Exome Variant Server (http://evs.gs. washington.edu/EVS/). Furthermore, we identified the *SLC7A9* mutation in DNA from the patient's urine (Fig. S3b).

On the basis of these findings we concluded that the patient was homozygous for the *SLC7A9* mutation in GWpUPD cells and heterozygous in biparental cells. Because a high ratio of mosaicism was found in the patient's urine (average mosaic rate: 76%) (Fig. S3a), we speculated that the high ratio of mosaicism also occurred in the patient's kidneys, which resulted in the observed cystinuria.

Discussion

In this study, we describe a patient concurrently afflicted with BWS and autosomal recessive cystinuria. Genetic analyses revealed that the patient, who possesses mosaic GWpUPD, is also homozygous for a *SLC7A9* mutation in GWpUPD cells, while her normal biparental cells are heterozygous. The mutation was inherited from the patient's father, who carried the mutation.

Approximately 20% of patients with BWS show mosaicism for pUPD11 (1). This segmental pUPD is considered to result from mitotic recombination at an early embryonic stage (11). A small number of reports exist that detail GWpUPD patients with BWS phenotypes (1). Fifteen patients with live-born mosaic GWpUPD, including our patient, have been described so far in 11 reports (Table 1) (4, 12–21). Although previous assumptions were of low GWpUPD incidence in pUPD11 patients, a recent report suggested that GWpUPD might actually be more frequent than expected because two GWpUPD patients were found out of 11 pUPD11 patients (22). All these patients showed only one paternal haplotype (isodisomy) and no evidence of any chromosomal crossing-over. This strongly suggests that a mechanism of mosaic GWpUPD involves normal fertilization followed by failure of maternal DNA replication and paternal genome endoreplication (12, 23, 24). These patients frequently show hyperinsulinemic hypoglycemia (12/15), often accompanied by nesidioblastosis, for which partial or near-total pancreatectomy may be required. The incidence of tumor development is much higher in GWpUPD patients (14/15) than in segmental pUPD11 (approximately 25%) (Table 1) (25). Several types of benign and malignant tumors develop metachronously and ectopically (12). Because segmental pUPD11 itself is a risk factor for tumor development, there may be additional factors in GWpUPD patients, such as as-yet poorly characterized imprinted regions and undiscovered recessive loci associated with cell growth or survival (12). The possibility of GWpUPD should be tested in patients with pUPD11 as a general, in particular to guard against their increased tumor risk.

Although other chromosomes, especially chromosomes 6, 14, 15, and 20, are also pUPD in GWpUPD patients, associated clinical features were seen less frequently with them, suggesting (epi)dominance of pUPD11 (Table 1). Yamazawa et al. suggested several determination factors for clinical features of mosaic GWpUPD, including the mosaic ratios in various tissues, dysregulation of imprinted domains, and unmasking of paternally inherited recessive mutations (4).

We found that our patient was homozygous for a one-base deletion mutation of *SLC7A9*, which is a causative gene for cystinuria. A GWpUPD patient has been previously reported to have renal calcium stones. However, the cause of the renal stones remains unknown (16). *SLC7A9* encodes $b^{+,0}$AT, which is a light subunit of the rBAT/$b^{0,+}$AT amino acid transporter expressed in the renal proximal tubule (5, 6). The mutation has been reported to decrease cystine transport activity drastically compared with wild-type rBAT/$b^{0,+}$AT *in vitro* (10). The loss of function of this transporter system leads to the formation of cystine stones in patients.

In conclusion, we report for the first time a patient concurrently affected by both BWS and autosomal recessive cystinuria. The genotype of this patient clearly indicates that a paternally inherited recessive mutation can cause a recessive disease in patients with mosaic GWpUPD. To understand the clinical conditions of patients with mosaic GWpUPD better, further investigation of dysregulation of imprinted domains and recessive mutations is necessary. To this end, whole exome sequencing would be useful in identifying paternally inherited recessive mutations.

Supporting Information

Additional supporting information may be found in the online version of this article at the publisher's web-site.

Acknowledgements

This study was supported, in part, by a Grant for Research on Intractable Diseases from the Ministry of Health, Labor, and Welfare; a Grant for Child Health and Development from the National Center for Child Health and Development; a Grant-in-Aid for Challenging Exploratory Research; and a Grant-in-Aid for Scientific Research (C) from the Japan Society for the Promotion of Science.

References

1. Choufani S, Shuman C, Weksberg R. Molecular findings in Beckwith-Wiedemann syndrome. Am J Med Genet C Semin Med Genet 2013: 163C: 131–140.
2. Soejima H, Higashimoto K. Epigenetic and genetic alterations of the imprinting disorder Beckwith-Wiedemann syndrome and related disorders. J Hum Genet 2013: 58: 402–409.
3. Romanelli V, Meneses HN, Fernández L et al. Beckwith-Wiedemann syndrome and uniparental disomy 11p: fine mapping of the recombination breakpoints and evaluation of several techniques. Eur J Hum Genet 2011: 19: 416–421.
4. Yamazawa K, Nakabayashi K, Matsuoka K et al. Androgenetic/biparental mosaicism in a girl with Beckwith-Wiedemann syndrome-like and upd(14)pat-like phenotypes. J Hum Genet 2011: 56: 91–93.
5. Barbosa M, Lopes A, Mota C et al. Clinical, biochemical and molecular characterization of cystinuria in a cohort of 12 patients. Clin Genet 2012: 81: 47–55.
6. Fotiadis D, Kanai Y, Palacín M. The SLC3 and SLC7 families of amino acid transporters. Mol Aspects Med 2013: 34: 139–158.
7. Weksberg R, Shuman C, Beckwith JB. Beckwith-Wiedemann syndrome. Eur J Hum Genet 2010: 18: 8–14.
8. Kubota A, Yonekura T, Usui N et al. Two cases of persistent hyperinsulinemic hypoglycemia that showed spontaneous regression and maturation of the Langerhans islets. J Pediatr Surg 2000: 35: 1661–1662.
9. Takama Y, Kubota A, Nakayama M et al. Fibroadenoma in Beckwith–Wiedemann syndrome with paternal uniparental disomy of chromosome 11p15.5. Pediatrics International 2014: in press.
10. Shigeta Y, Kanai Y, Chairoungdua A et al. A novel missense mutation of SLC7A9 frequent in Japanese cystinuria cases affecting the C-terminus of the transporter. Kidney Int 2006: 69: 1198–1206.
11. Yamazawa K, Nakabayashi K, Kagami M et al. Parthenogenetic chimaerism/mosaicism with a Silver-Russell syndrome-like phenotype. J Med Genet 2010: 47: 782–785.
12. Kalish JM, Conlin LK, Bhatti TR et al. Clinical features of three girls with mosaic genome-wide paternal uniparental isodisomy. Am J Med Genet A 2013: 161A: 1929–1939.
13. Johnson JP, Waterson J, Schwanke C et al. Genome-wide androgenetic mosaicism. Clin Genet 2014: 85: 282–285.
14. Inbar-Feigenberg M, Choufani S, Cytrynbaum C et al. Mosaicism for genome-wide paternal uniparental disomy with features of multiple imprinting disorders: diagnostic and management issues. Am J Med Genet A 2013: 161A: 13–20.
15. Gogiel M, Begemann M, Spengler S et al. Genome-wide paternal uniparental disomy mosaicism in a woman with Beckwith-Wiedemann syndrome and ovarian steroid cell tumour. Eur J Hum Genet 2013: 21: 788–791.
16. Romanelli V, Nevado J, Fraga M et al. Constitutional mosaic genome-wide uniparental disomy due to diploidisation: an unusual cancer-predisposing mechanism. J Med Genet 2011: 48: 212–216.
17. Wilson M, Peters G, Bennetts B et al. The clinical phenotype of mosaicism for genome-wide paternal uniparental disomy: two new reports. Am J Med Genet A 2008: 146A: 137–148.
18. Reed RC, Beischel L, Schoof J et al. Androgenetic/biparental mosaicism in an infant with hepatic mesenchymal hamartoma and placental mesenchymal dysplasia. Pediatr Dev Pathol 2008: 11: 377–383.
19. Giurgea I, Sanlaville D, Fournet JC et al. Congenital hyperinsulinism and mosaic abnormalities of the ploidy. J Med Genet 2006: 43: 248–254.
20. Bryke C, Garber A, Israel J. Evolution of a complex phenotype in a unique patient with a paternal uniparental disomy for every chromosome cell line and a normal biparental inheritance cell line. Toronto, Canada: The annual meeting of The American Society of Human Genetics, 2004: Program Number: 823.
21. Hoban PR, Heighway J, White GR et al. Genome-wide loss of maternal alleles in a nephrogenic rest and Wilms' tumour from a BWS patient. Hum Genet 1995: 95: 651–656.
22. Eggermann T, Heilsberg AK, Bens S et al. Additional molecular findings in 11p15-associated imprinting disorders: an urgent need for multi-locus testing. J Mol Med (Berl) 2014: 92: 769–777.
23. Kotzot D. Complex and segmental uniparental disomy updated. J Med Genet 2008: 45: 545–556.
24. Lapunzina P, Monk D. The consequences of uniparental disomy and copy number neutral loss-of-heterozygosity during human development and cancer. Biol Cell 2011: 103: 303–317.
25. Choufani S, Shuman C, Weksberg R. Beckwith-Wiedemann syndrome. Am J Med Genet C Semin Med Genet 2010: 154C: 343–354.

nature COMMUNICATIONS

ARTICLE

Received 8 Oct 2013 | Accepted 30 Apr 2014 | Published 2 Jun 2014

DOI: 10.1038/ncomms5011

De novo SOX11 mutations cause Coffin–Siris syndrome

Yoshinori Tsurusaki[1,*], Eriko Koshimizu[1,*], Hirofumi Ohashi[2], Shubha Phadke[3], Ikuyo Kou[4], Masaaki Shiina[5], Toshifumi Suzuki[1,6], Nobuhiko Okamoto[7], Shintaro Imamura[8], Michiaki Yamashita[8], Satoshi Watanabe[9], Koh-ichiro Yoshiura[9], Hirofumi Kodera[1], Satoko Miyatake[1], Mitsuko Nakashima[1], Hirotomo Saitsu[1], Kazuhiro Ogata[5], Shiro Ikegawa[4], Noriko Miyake[1] & Naomichi Matsumoto[1]

Coffin–Siris syndrome (CSS) is a congenital disorder characterized by growth deficiency, intellectual disability, microcephaly, characteristic facial features and hypoplastic nails of the fifth fingers and/or toes. We previously identified mutations in five genes encoding subunits of the BAF complex, in 55% of CSS patients. Here we perform whole-exome sequencing in additional CSS patients, identifying *de novo SOX11* mutations in two patients with a mild CSS phenotype. *sox11a/b* knockdown in zebrafish causes brain abnormalities, potentially explaining the brain phenotype of CSS. SOX11 is the downstream transcriptional factor of the PAX6–BAF complex, highlighting the importance of the BAF complex and SOX11 transcriptional network in brain development.

[1] Department of Human Genetics, Yokohama City University Graduate School of Medicine, 3-9 Fukuura, Kanazawa-ku, Yokohama 236-0004, Japan. [2] Division of Medical Genetics, Saitama Children's Medical Center, 2100 Magome, Iwatsuki 339-8551, Japan. [3] Department of Medical Genetics, Sanjay Gandhi Postgraduate Institute of Medical Sciences, Raebareli Rd, Lucknow 226014, India. [4] Laboratory for Bone and Joint Diseases, Center for Integrative Medical Sciences, RIKEN, 4-6-1 Shirokanedai, Minato-ku, Tokyo 108-8639, Japan. [5] Department of Biochemistry, Yokohama City University Graduate School of Medicine, 3-9 Fukuura, Kanazawa-ku, Yokohama 236-0004, Japan. [6] Department of Obstetrics and Gynecology, Juntendo University, Hongo 3-1-3, Bunkyo-ku, Tokyo 113-8431, Japan. [7] Department of Medical Genetics, Osaka Medical Center and Research Institute for Maternal and Child Health, 840 Murodo-cho, Izumi 594-1101, Japan. [8] National Research Institute of Fisheries Science, 2-12-4 Fukuura, Kanazawa-ku, Yokohama 236-8648, Japan. [9] Department of Human Genetics, Nagasaki University Graduate School of Biomedical Sciences, 1-12-4 Sakamoto, Nagasaki 852-8523, Japan. * These authors contributed equally to this work. Correspondence and requests for materials should be addressed to N.M. (email: naomat@yokohama-cu.ac.jp).

Coffin–Siris syndrome (CSS; MIM#135900) is a congenital disorder characterized by growth deficiency, intellectual disability, microcephaly, characteristic facial features and hypoplastic nails of the fifth fingers and/or toes (Supplementary Fig. 1). Five subunit genes (*SMARCB1*, *SMARCA4*, *SMARCE1*, *ARID1A* and *ARID1B*) of the BAF complex (also known in yeast as the SWI/SNF complex[1]) are mutated in 55–70% of CSS patients[2–6]. Mutations in *SMARCA2*, another BAF complex gene, were reported in the Nicolaides–Baraitser syndrome, which is similar to, but distinct from CSS[7]. Furthermore, *de novo PHF6* mutations were found in two CSS patients[6], although no direct interaction has been reported between the BAF complex and PHF6, which interacts with the nucleosome remodelling and deacetylation complex[6]. As 30–45% of CSS patients were genetically undiagnosed in three large cohort studies[2–6], further genetic investigation is required to fully address the genetic picture of CSS.

Here we apply whole-exome sequencing (WES) to 92 CSS patients, and identify two *de novo SOX11* mutations in two unrelated patients. *sox11* knockdown experiments in zebrafish result in a smaller head and significant mortality, which were partially rescued by human wild-type *SOX11* messenger RNA (mRNA), but not by mutant mRNA.

Results

WES of CSS patients. We identified two *de novo SOX11* mutations in two unrelated patients, c.347A>G (p.Tyr116Cys) (in patient 1) and c.178T>C (p.Ser60Pro) (in patient 2) (deposited to LOVD, http://www.LOVD.nl/SOX11), among 92 CSS patients (including our previous cohorts[2,3]) analysed by trio-based WES. In the two patients, >10 reads covered 94–92% of coding sequences and only *SOX11* mutations remained as candidate variants in both of them based on the *de novo* model with scores of damaging or disease causing by SIFT, PolyPhen2 and Mutation Taster (Supplementary Table 1). The two heterozygous mutations localize to the high-mobility group (HMG) domain. Neither mutation was registered in the databases examined (1,000 Genomes, Exome Sequencing project (ESP) 6500, and in-house databases containing 575 control exomes) (Supplementary Table 1). We identified a further 22 *SOX11* variants within these three databases, but all of them reside outside the HMG domain and, based on prediction programs, are less likely to be pathogenic (Supplementary Table 1; Supplementary Fig. 2). The amino acids altered in SOX11 are evolutionarily conserved from zebrafish to human (Fig. 1). The mutations do not alter nuclear localization of SOX11 protein (Supplementary Fig. 3). *De novo* mutations were confirmed in the two families by Sanger sequencing along with biological parentage. No mutations in any of the other BAF complex genes, *PHF6*, or other potential candidate genes were found in the two families. Therefore, the two mutations identified are highly likely to be pathogenic. Moreover, *SOX11* was sequenced by WES ($n=23$) or Sanger method ($n=67$) in a further 90 CSS patients, with no mutations found. Fifty-four patients had a mutation in one of the five BAF complex subunit genes (58.7%) (*SMARCA4, SMARCB1, SMARCE1, ARID1A* and *ARID1B* mutations found in 9, 8, 1, 5 and 31 patients, respectively).

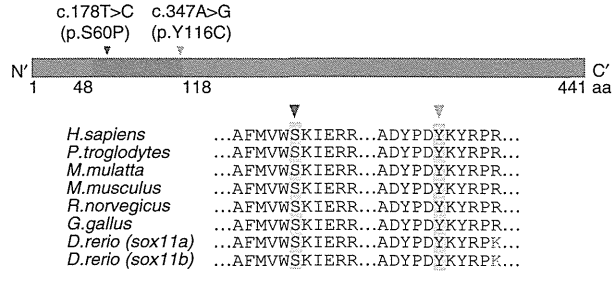

Figure 1 | *SOX11* mutations and functional characterization. *SOX11* mutations in CSS patients. Two missense mutations in the HMG domain (blue box) occur at evolutionarily conserved amino acids.

Clinical features of patients with *SOX11* mutations. The two patients showed dysmorphic facial features, microcephaly, growth deficiency, hypoplastic fifth toe nails and mild intellectual disability[8] (Supplementary Fig. 1; Supplementary Table 2). The observed clinical features in both patients are classified to a mild end of CSS as patient 1 spoke early for CSS and patient 2 has relatively high intelligence quotient. Although the two patients do not look similar in facial appearance (patient 1 has midface hypoplasia, while patient 2 does not; in addition there is an ethnic difference, as patients were either Japanese or Indian), they do share features in common, namely, hypertrichosis, arched eyebrows, low-set ears, auricular back-rotationand full cheeks (Supplementary Fig. 1).

Patient 1 (Japanese) was born at 38 weeks of gestation following an uneventful pregnancy. Her birth weight was 2,340 *g* (−1.9 s.d.), length 45 cm (−2.2 s.d.) and occipitofrontal circumference (OFC) 30.5 cm (−1.8 s.d.). She was hypotonic, had feeding difficulties (especially during the neonatal period) and delayed development. She was able to support her head at 5 months of age, sit at 11 months and walk independently at 1 year 11 months. She started to speak meaningful words at 1 year 7 months. At 3 years, her developmental quotient was estimated using the Kyoto scale of psychological development to be 57. Abdominal echography showed her left kidney was slightly small in size. She has distinctive facial features characterized by midface hypoplasia, short palpebral fissures, hypertelorism, upturned palpebral fissures, long eyelashes, a low nasal root, shortened nose with upturned nostrils, short philtrum, open mouth, full lips and low-set ears. Hypoplastic distal phalanges with nail hypoplasia (especially of the fifth digits) were also noted. Additional findings included hypertrichosis and long eyelashes with abundant hair on the scalp. At 4 years 8 months, she was short with a height of 92.1 cm (−2.9 s.d.) and evaluated for possible growth hormone deficiency with stimulation tests, which showed normal results. At 10 years, she measured 119 cm (−2.8 s.d.), weighed 20.1 kg (−1.8 s.d.) and had an OFC of 47.3 cm (−3.3 s.d.). She attends a special education class for poor performance, but can walk to school by herself (takes approximately half an hour) and is able to communicate verbally, to some extent, with her classmates. Clinical features are summarized in Supplementary Table 2.

Patient 2 (Indian) is a 16-year-old female, and was referred to the genetics outpatient department for evaluation of short stature. She was born at term following a normal pregnancy, but with low birth weight (1.75 kg, −4s.d.). Developmental milestones were attained normally, but her parents always felt that she lagged behind other children. She was a slow learner with poor scholastic performance and an intelligence quotient of 70–80. She attended a normal class, but struggled to pass class examinations every year. She has a proportionately short stature but not a coarse face. Her chin was small and supraorbital ridges hypoplastic with no ptosis. Her nose was long and alae nasi hypoplastic with overhanging columella. Her hair was thick and rough with some thinning on her scalp. She had increased hair on her back. Her fourth and fifth toes were short and all her finger nails were hypoplastic with thin and tapered fingers. Her fourth and fifth toes on both feet, and also the third toe on her right foot, were

markedly hypoplastic. Clinodactyly was noted on the third, fourth and fifth toes on her right foot, and the third and fourth toes on her left foot. A skeletal survey did not show any radiographic bone abnormalities. Her bone age was 13–14 years and follicle-stimulating hormone was $1.57\,IU\,l^{-1}$ (normal range: $<5\,IU\,l^{-1}$). Ultrasonographic examination at 16 years (before menarche), showed a hypoplastic uterus and malrotation of both kidneys. No secondary sexual characteristics were recognized until she had menarche at 17 years. Now at age of 17 years, she is still short with a height of 141 cm (-5 s.d.), weigh 31.3 kg (-3 s.d.) and OFC 50.5 cm (-4.5 s.d.). Clinical features are summarized in Supplementary Table 2.

Structural effects of SOX11 mutations. To determine the impact of the disease-causing mutations on human SOX11 structure and function, we mapped the mutation positions onto the crystal structure of mouse Sox4[9], that is analogous to human SOX11, and calculated free energy changes on the mutations using FoldX software[10,11]. The mutations lie in the highly conserved HMG domain, responsible for sequence-specific DNA binding (Fig. 2a)[9]. Ser60 is located in a helix of the HMG domain (Fig. 2a), therefore the S60P mutation may affect overall folding of the HMG domain and impair DNA binding of SOX11. FoldX calculations supported this prediction and the free energy change on the mutation was high enough to destabilize protein folding ($>10\,kcal\,mol^{-1}$) (Fig. 2b)[12]. Conversely, Tyr116 forms a hydrophobic core with the side chains of DNA-recognition loops (Fig. 2a). The Y116C mutation has low free energy change ($<1\,kcal\,mol^{-1}$) (Fig. 2b), and is unlikely to significantly affect folding of the HMG domain, but instead may alter conformation of the DNA-recognition loop, which is important for DNA binding.

***SOX11* mutations affect downstream transcription.** Both mutations are located within the HMG domain, which is required for *SOX11* transcriptional regulation of *GDF5* (ref. 13). Luciferase assays using the *GDF5* promoter in HeLa and ATDC5 cells, showed both mutant proteins had decreased transcriptional activities compared with wild type (WT) (Fig. 3).

SOX11 expression. *SOX11* transcription levels were examined using multiple human complementary DNA (cDNA) panels. *SOX11* was exclusively expressed in brain (foetus and adult) and heart (adult) tissues, supporting a role for *SOX11* mutations in the brain features of CSS observed in the two patients (Supplementary Fig. 4; Supplementary Table 2).

In mice, targeted *Sox11* disruption with a β-galactosidase marker gene results in 23% birth weight reduction and lethality after the first postnatal week in homozygotes, due to hypoplastic lungs and ventricular septation defects. In addition, skeletal malformations (including phalanges) and abdominal defects are observed[14]. Physical and functional abnormalities in heterozygotes have not been described. However, in heterozygous mice, β-galactosidase expression revealed early ubiquitous expression throughout the embryo with upregulation in the central nervous system (CNS) and limb buds[14].

***sox11* knockdown experiments in zebrafish.** We further investigated *sox11* function in zebrafish. The zebrafish genome contains two orthologs of human *SOX11*, *sox11a* and *sox11b*, which are expressed in all cells until gastrulation and later become restricted to the developing CNS[15,16]. We knocked down zebrafish *sox11a* and *sox11b* (both single-exon genes) using translation-blocking morpholino oligonucleotides (MOs) (*sox11a*-MO, *sox11b*-MO and *sox11a/b*-MO), as previously described[17] (Supplementary Fig. 5a). Off-target effects of morpholino injections were excluded by repeated experiments, co-injecting with *tp53* MO or injecting into *tp53*$^{zdf1/zdf1}$ mutant fish[18,19]. *sox11a*- and *sox11b*-MO knockdown caused similar phenotypes, including smaller heads and body curvature (Supplementary Fig. 5b). Low-dose *sox11a*- (1.6 ng), *sox11b*- (1.6 ng) and *sox11a/b*- (1.6 ng) MO-injected embryos resulted in

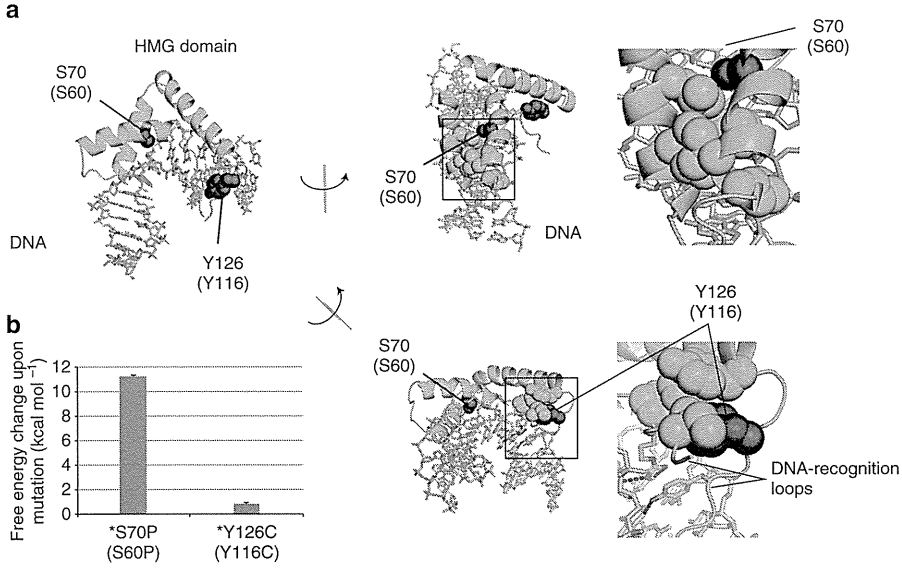

Figure 2 | Structural effects of SOX11 mutations. (**a**) Crystal structure of the mouse Sox4 HMG domain bound to DNA. Helices and loops are shown as green ribbons and threads, respectively. DNA is shown as grey sticks. Amino-acid residues at mutation sites are shown coloured red in the space-filling model. In the middle and right images, some of the amino-acid residues involved in the hydrophobic core surrounding mutation points are shown coloured green in the space-filling model. Amino-acid numbering is indicated for mouse Sox4 with that for human SOX11 in parentheses. Hydrogen bonds are shown as black dotted lines. Molecular structures were drawn using PyMOL (http://www.pymol.org). (**b**) Free energy changes on the indicated mutations calculated by FoldX software.

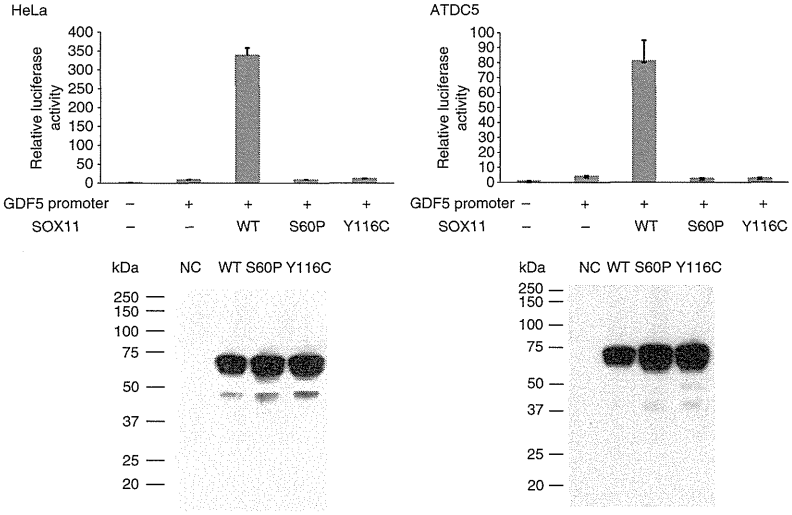

Figure 3 | *SOX11* mutations affecting *GDF5* promoter activity. Luciferase reporter assays measured transcriptional activity of the *GDF5* promoter (−448/+319) (UCSC genome browser hg19: chr20: 34025709-34026457) in HeLa (left) and ATDC5 (right) cells. HeLa or ATDC5 cells were co-transfected with WT or mutant (S60P and Y116C) SOX11 expression vector and reporter constructs containing either GDF5 promoter or empty vector (pGL3-basic). Relative luciferase activities compared with empty vector are presented as mean ± s.d. for two independent experiments, with each experiment performed in triplicate (upper). Immunoblot analysis of transfected HeLa and ATDC5 cell extracts showing wild-type (WT) or mutant (S60P and Y116C) SOX11 proteins (lower). Compared with WT, both SOX11 mutants reduced *GDF5* transcriptional activities in HeLa and ATDC5 cells.

significant mortality (*sox11a*-MO, ~49.3%; *sox11b*-MO, ~19.3%; *sox11a/b*-MO, ~53.0%), compared with control-MO embryos (~7.3%) (Fig. 4a). Co-injection of WT human *SOX11* mRNA (h*SOX11*-WT mRNA) with *sox11a/b*-MO improved morphant survival at 48 h post fertilization (hpf) (25.5% lethality versus 49.3% lethality with *sox11a/b*-MO alone) ($P<0.01$) (Fig. 4a; Supplementary Fig. 5c). The affected phenotype of *sox11a/b* double morphants was partially rescued by h*SOX11*-WT mRNA overexpression (4.5% normal for *sox11a/b*-MO alone versus 36.5% for co-injection with h*SOX11*-WT mRNA and *sox11a/b*-MO, $P<0.01$) (Fig. 4a). In contrast, co-injection of either mutant h*SOX11* mRNA (h*SOX11*-S60P and -Y116C mRNA) with *sox11a/b*-MO showed no significant rescue effects on lethal and affected phenotypes (Fig. 4a). There were significantly more normal phenotypes following h*SOX11*-WT mRNA and *sox11a/b*-MO co-injection, than with h*SOX11*-mutant mRNA co-injections ($P<0.05$). Head sizes in randomly selected embryos ($n\geq10$) of *sox11a* and *sox11a/b* morphants at 48 hpf were significantly decreased ($P<0.05$ in both), but not significantly changed in *sox11b* morphant. Overexpression of h*SOX11*-WT mRNA restores *sox11a/b* double-morphant head size (in randomly selected embryos, $n\geq10$), suggesting specific *sox11* suppression by morpholino injection (Fig. 4b). Although the head size of h*SOX11*-mutant mRNA and *sox11a/b*-MO-injected embryos was slightly decreased, no significant difference was recognized between overexpression of h*SOX11*-WT or h*SOX11*-mutant mRNA and *sox11a/b*-MO co-injection (Fig. 4b).Staining with acridine orange and terminal deoxynucleotidyl TdT-mediated dUTP nick end labelling (TUNEL), found significant apoptotic increases exclusively in microcephalic embryos (Fig. 4c; Supplementary Fig. 6). Brain cell death was prevented by co-injection with h*SOX11*-WT mRNA, but not by mutant h*SOX11* mRNAs (Fig. 4c). We also used HuC/D (a marker for early postmitotic and mature neurons) and acetylated tubulin (an axonal marker) immunostaining at 48 hpf to analyse neuronal cells in more detail (Supplementary Fig. 7). Decreased HuC/D-positive neurons, especially in the telencephalon and diencephalon, were observed in *sox11* morphants (Supplementary Fig. 7a). The phenotype in *sox11a/b*-MO-injected embryos was efficiently rescued by h*SOX11*-WT mRNA (Supplementary Fig. 7a). Reduction of HuC/D-positive neurons was unaltered by mutant h*SOX11* mRNA overexpression and *sox11a/b*-MO injection (Supplementary Fig. 7a). Anti-acetylated tubulin staining also showed severely reduced axonal numbers in the forebrain, midbrain and hindbrain of *sox11* morphants, compared with control-MO-injected embryos (Supplementary Fig. 7b). *sox11a/b* morphants showed phenotypic rescue when co-injected with h*SOX11*-WT mRNA, compared with mutant h*SOX11* mRNAs (Supplementary Fig. 7b).

Discussion

We have identified *SOX11* mutations in CSS. This is the first report of human mutations in *SOXC* (*SOX4*, *SOX11* and *SOX12*)[20]. *SOX11/sox11* is required for neurogenesis, and loss of function in early embryos is sufficient to impair normal CNS development. Haploinsufficiency of other *SOX* genes (*SOX2*, *SOX9* and *SOX10*) is known to cause human diseases[21–23]. It is interesting that mutations of *SOX11* and other BAF subunit genes are mutually exclusive in CSS.

Sox11 was recently shown to form a transcriptional cross-regulatory network downstream of the Pax6–BAF complex. The network drives neurogenesis and converts postnatal glia into neurons[24]. Brg1 (Smarca4) binds to the *Sox11* promoter, and interaction with Pax6 is sufficient to induce Sox11 expression in neurosphere-derived cells in a Brg1-dependent manner[24]. Therefore, the Pax6–BAF complex activates a cross-regulatory transcriptional network, maintaining high expression of genes involved in neuronal differentiation and execution of cell lineage decisions[24]. *SOX11* mutations appear to be a rare cause of CSS as only 2 out of 92 patients (2.2%) showed *SOX11* abnormality and to be limited to the mild end of CSS phenotype. Abnormality of the upstream BAF complex tends to show a more severe phenotype compared with that of a downstream *SOX11* mutation, which may indicate rather specific effects of *SOX11* mutations on the CSS phenotype.